UNIVERSITY OF BARI ALDO MORO

PhD programme in Transplantation of Tissues and Organs and Cellular Therapies

IDENTIFICATION OF IRISIN RECEPTOR IN PANCREATIC β-CELLS

Department of Precision and Regenerative Medicine and Ionian Area (DiMePRe-J)
Section of Internal Medicine, Endocrinology, Andrology and Metabolic Diseases

Supervisor:

Prof. Annalisa Natalicchio

Co-supervisor:

Dr. Nicola Marrano

PhD student:

Dr. Martina Rella

XXXVIII CYCLE

Oral presentations at national and international scientific conferences

- ***61st EASD Annual Meeting, Vienna 15-19 September, 2025***

Identification of Irisin Receptor in Pancreatic β-Cells

Martina Rella[1], Nicola Marrano[1], Giuseppina Biondi[1], Valerio Galasso[1], Giovanni Galluzzi[1], Angelo Cignarelli[1], Sebastio Perrini[2], Luigi Laviola[1], Francesco Giorgino[1], and Annalisa Natalicchio[1]

[1]Department of Precision and Regenerative Medicine and Ionian Area, University of Bari Aldo Moro, Bari, Italy

[2]Section of Endocrinology, Department of Medicine and Surgery, LUM University, Casamassima, Bari, Italy

Background and Aims

Irisin is a myokine secreted by skeletal muscle in response to physical activity and a diet rich in saturated fats, derived from the proteolytic cleavage of the membrane protein FNDC5 (fibronectin type III domain-containing protein 5). Irisin is known to improve metabolic homeostasis and promote energy expenditure by acting on various tissues and organs, thereby regulating multiple metabolic pathways. We previously demonstrated that irisin protects pancreatic β-cells and islets from lipotoxicity-induced apoptosis, increases insulin biosynthesis, enhances glucose-stimulated insulin secretion (GSIS), and promotes β-cell proliferation both in vitro and in vivo, in mice. Moreover, circulating irisin levels are significantly reduced in patients with type 2 diabetes (T2DM) compared to controls, and irisin has been shown to restore β-cell functional deficit in these patients. While irisin effects on bone and adipose tissue are mediated through αV integrin receptors, the presence of an irisin receptor in pancreatic β-cells has not yet been reported.

Materials and Methods

In INS-1E rat insulinoma cells, we found that irisin activates intracellular signaling and enhances GSIS even in the presence of a specific αV integrin knockdown or a chemical inhibitor of integrins (RGDS), thereby excluding the involvement of integrin receptors in irisin effects on pancreatic β-cells. Additionally, irisin does not activate focal adhesion kinase (FAK), the main intracellular mediator of integrin-activated signaling. Using a pull-down/mass spectrometry approach, we identified 102 irisin interactors in human pancreatic islets, most of which are associated with intracellular compartments and do not include canonical membrane receptors. Based on these findings, we hypothesized that irisin undergoes endocytosis in pancreatic β-cells, and we confirmed this through immunoblot analysis of intracellular proteins and immunofluorescence assays. Furthermore, both nystatin, an inhibitor of lipid

raft-mediated endocytosis, and heat denaturation of irisin, a strategy to block protein endocytosis, interfered with irisin internalization in pancreatic β-cells. To investigate the role of endocytosis in irisin biological effect, we used a His-tagged irisin and found that it is not endocytosed and does not enhance GSIS in INS-1E cells. Lastly, using the novel Ligand-Receptor-Capture-TriCEPS (LRC-TriCEPS) technology, we aimed to identify a membrane-anchored protein that might mediate irisin endocytosis. Preliminary results show that irisin anchors the plasma membrane of β-cells before being endocytosed.

Results

These findings demonstrate that irisin effects on pancreatic β-cells are independent of integrin αV receptor engagement.

Conclusions

The inability of His-tagged irisin, which is not endocytosed, to enhance GSIS, suggests for the first time that irisin biological effect on pancreatic β-cells are dependent on its endocytosis.

- ***43 rd National Congress of the Italian Society of Endocrinology, Turin, June 11-14, 2025***

Identificazione del recettore della miochina irisina nelle β-cellule pancreatiche

Martina Rella [1], Nicola Marrano[1], Giuseppina Biondi[1], Valerio Galasso[1], Giovanni Galluzzi[1], Angelo Cignarelli[1], Sebastio Perrini[2], Luigi Laviola[1], Francesco Giorgino[1], and Annalisa Natalicchio[1].

[1]Dipartimento di Medicina di Precisione e Rigenerativa e Area Jonica, Università degli Studi di Bari Aldo Moro, Bari.

[2]Sezione di Endocrinologia, Dipartimento di Medicina e Chirurgia, Università LUM, Casamassima, Bari.

L'irisina è una miochina secreta dal muscolo scheletrico in risposta all'attività fisica e a una dieta ricca di grassi saturi, in grado di favorire l'omeostasi metabolica. Abbiamo precedentemente dimostrato che l'irisina protegge le β-cellule e le isole pancreatiche dall'apoptosi indotta dalla lipotossicità, incrementa la biosintesi di insulina e la secrezione insulinica glucosio-stimolata (GSIS) e promuove la proliferazione β-cellulare. L'irisina è anche in grado di ripristinare il deficit funzionale β-cellulare, tipico delle isole di pazienti affetti da diabete mellito di tipo 2. Sebbene sia stato dimostrato che l'irisina medi i suoi effetti sul tessuto osseo e adiposo tramite il recettore integrinico αV, ad oggi non è noto quale sia il recettore dell'irisina nelle β-cellule pancreatiche.

Nelle cellule di insulinoma di ratto INS-1E, l'irisina si è dimostrata in grado di attivare il signalling intracellulare e promuovere la GSIS anche in presenza del knockdown dell'espressione dell'integrina αV e di un inibitore chimico delle integrine cellulari, escludendo il coinvolgimento dei recettori integrinici negli effetti β-cellulari dell'irisina. Inoltre, l'irisina non ha indotto l'attivazione di FAK, principale mediatore intracellulare del pathway integrinico. Attraverso un approccio di pull-down assay/spettrometria di massa su isole pancreatiche umane, abbiamo identificato 102 proteine co-eluite in modo specifico con l'irisina e abbiamo verificato che la maggior parte di esse erano localizzate in compartimenti intracellulari e nessuna aveva funzioni recettoriali canoniche. Abbiamo quindi ipotizzato che l'irisina sia endocitata nelle β-cellule pancreatiche, confermando tale ipotesi tramite analisi di immunoblotting delle proteine intracellulari e saggi di immunofluorescenza. Inoltre, sia la nistatina, un inibitore dell'endocitosi mediata da lipid-raft, sia la denaturazione dell'irisina con il calore, una strategia per inibire l'endocitosi delle proteine, hanno interferito con il processo di internalizzazione dell'irisina nelle β-cellule pancreatiche. Per studiare il ruolo dell'endocitosi negli effetti biologici dell'irisina, abbiamo verificato che l'irisina His-tag, che non viene endocitata, non è in grado di promuovere la GSIS in modo paragonabile all'irisina ricombinante non taggata. Attraverso la moderna tecnologia Ligand-Receptor-Capture-TriCEPS abbiamo cercato di individuare l'esistenza di una proteina di aggancio alla membrana in grado di mediare l'endocitosi. Come dimostrato da test preliminari, l'irisina è in grado di agganciarsi alla membrana plasmatica prima di essere endocitata.

Questi risultati dimostrano che gli effetti dell'irisina sulle β-cellule sono indipendenti dal coinvolgimento del recettore integrinico αV. Il dato che l'irisina His-tag, che non viene endocitata, non è più in grado di promuovere la GSIS, suggerisce per la prima volta che i suoi effetti sulla β-cellula pancreatica sono secondari all'endocitosi.

- *10th Spring Meeting Congress, Rimini, April 6-8, 2025*

Irisin Restores the Secretory Function of Pancreatic β-Cells in Experimental and Human T2D

Martina Rella[1], Anna Borrelli[1], Nicola Marrano[1], Giuseppina Biondi[1], Luca Roberto[2], Leonardo Vincenti[3], Federico Baruzzi[4], Piero Marchetti[5], Lorenzo Piemonti[6], Angelo Cignarelli[1], Sebastio Perrini[1], Luigi Laviola[1], Francesco Giorgino[1], and Annalisa Natalicchio[1].
[1]Department of Precision and Regenerative Medicine and Ionian Area, Section of Internal Medicine, Endocrinology, Andrology and Metabolic Diseases, University of Bari Aldo Moro, Bari, Italy.
[2]Transgenic Mice Facility, Biogem S.c.a.r.l., Ariano Irpino (AV), Italy.
[3]General Surgery Unit, National Institute of Gastroenterology "Saverio de Bellis", Research Hospital, Castellana Grotte, Bari, Italy.
[4]National Research Council, Institute of Sciences of Food Production (CNR-ISPA), Bari, Italy.
[5]Department of Clinical and Experimental Medicine, University of Pisa, Pisa, Italy.
[6]Diabetes Research Institute, IRCCS San Raffaele Hospital, Milan, Italy.

Aim:
In this study, the effects of irisin, a hormone secreted by skeletal muscle, able to improve metabolic homeostasis and promote energy expenditure, on the β-cell functional mass were evaluated both in diabetic mice in vivo and in human pancreatic islets isolated from subjects with type 2 diabetes (T2D) ex vivo. Moreover, the molecular mechanisms underlying irisin action were investigated.

Methods:
C57Bl/6 mice (n=8) were made diabetic by a high-fat diet (HFD) and a single-dose of streptozotocin (STZ). 4 standard diet (SD)-fed mice were used as control. HFD/STZ mice were daily treated with 0.5 μg/g irisin (n=4) or vehicle (n=4) for 14 days. Fasting glycemia, insulinemia, body weight, glucose tolerance, and glucose-stimulated insulin secretion (GSIS) were assessed. Pancreatic islet architecture and β-cell apoptosis/proliferation were evaluated by immunofluorescence analyses. Pancreatic islets isolated from T2D patients (n=14) and non-diabetic subjects (ND) (n=10), as well as INS-1E cells, were exposed to 100 nM irisin for different times. GSIS and insulin content were measured by ELISA assays; intracellular signaling proteins and calcium levels were evaluated by immunoblotting and fluorimetric assay, respectively.

Results:
Irisin administration improved glycemic homeostasis, reduced body weight, and increased β-cell functional mass by stimulating β-cell proliferation and enhancing GSIS in vivo. Moreover, in T2D islets irisin augmented insulin content and GSIS. Of note, irisin activated CREB and AKT in INS-1E cells under physiological conditions, but not under glucotoxic conditions. However,

while chronic exposure to excess glucose blunted both GSIS and glucose-evoked increase in cytoplasmic calcium levels, irisin restored insulin secretion through the mobilization of calcium stores from the endoplasmic reticulum (ER).

Conclusions:
These findings highlight the role of irisin as a hormone that counteracts β-cell failure under dysmetabolic conditions in both rodents and humans and could be used to delay T2D onset and/or progression.

- **3rd EnGioI National Congress, Turin, January 24–25, 2025**

Identification of myokine irisin receptor in pancreatic β-cells

Martina Rella [1], Nicola Marrano[1], Anna Borrelli[1], Giuseppina Biondi[1], Angelo Cignarelli[1], Sebastio Perrini[1], Luigi Laviola[1], Francesco Giorgino[1], and Annalisa Natalicchio[1].

[1]Department of Precision and Regenerative Medicine and Ionian Area, Section of Internal Medicine, Endocrinology, Andrology and Metabolic Diseases, University of Bari Aldo Moro, Bari, Italy.

Background and aim: We have previously demonstrated that irisin, a hormone secreted by skeletal muscle, protects human and rodent β-cells and pancreatic islets from lipotoxicity-induced apoptosis, increases insulin biosynthesis and glucose-stimulated insulin secretion (GSIS), and promotes β-cell proliferation, both in vitro and in vivo in mice. Although it has been demonstrated that irisin mediates its effects on bone and adipose tissue via αV integrin receptors, the presence of an irisin receptor in β-cells has not been reported.

Materials and methods: INS-1E rat insulinoma cells were treated with 30 nM αV integrin siRNA for 24 h or 1 μM RGDS (a chemical inhibitor of cellular integrins) for 10 min, and then exposed to 100 nM irisin for different times. Under these conditions, intracellular signalling and GSIS were evaluated by immunoblotting and insulin ELISA assay, respectively. In human pancreatic islets, irisin interactome was assessed through a pull-down assay/mass spectrometry approach. Irisin endocytosis was evaluated by immunoblotting and immunofluorescence techniques, in INS-1E cells stimulated with 100 nM recombinant irisin or heat-denatured irisin. Furthermore, INS-1E cells were exposed to 53 μM nystatin (an inhibitor of lipid-raft dependent endocytosis) for 1 h, and then stimulated with 100 nM irisin for 15 min. Moreover, GSIS was assessed in INS-1E cells treated with 100 nM his-tag irisin, that is not endocytosed.

Results: In INS-1E cells, we found that irisin activates its intracellular signalling and enhances GSIS in the presence of αV integrin knockdown or RGDS, thus

excluding the involvement of integrin receptors in irisin effects. In human pancreatic islets, we identified 102 irisin interactors, mostly belonging to intracellular compartments. We therefore hypothesized that irisin could be endocytosed in pancreatic β-cells and confirmed this by immunoblotting and immunofluorescence techniques. In addition, since heat-induced denaturation prevents the entry of proteins into cells by endocytosis, we demonstrated that denatured irisin was unable to entry into INS-1E cells. Furthermore, nystatin reduced irisin entry into pancreatic β-cells. Moreover, unlike untagged irisin, his-tag irisin was not able to promote GSIS.

Conclusion: These results suggest for the first time that irisin effects on pancreatic β-cells are independent of engaging the αV integrin receptor. To date, we found that irisin may not recognize canonical membrane receptors and is instead endocytosed in INS-1E cells.

- **30th National Congress of the Italian Society of Diabetology, Rimini, October 23–26, 2024**

Identification of myokine irisin receptor in pancreatic β-cells

Martina Rella [1], Nicola Marrano[1], Anna Borrelli[1], Giuseppina Biondi[1], Angelo Cignarelli[1], Sebastio Perrini[1], Luigi Laviola[1], Francesco Giorgino[1], and Annalisa Natalicchio[1].

[1]Department of Precision and Regenerative Medicine and Ionian Area, Section of Internal Medicine, Endocrinology, Andrology and Metabolic Diseases, University of Bari Aldo Moro, Bari, Italy.

We have previously demonstrated that irisin, a hormone secreted by skeletal muscle, protects human and rodent β-cells and pancreatic islets from lipotoxicity-induced apoptosis, increases insulin biosynthesis and glucose-stimulated insulin secretion (GSIS), and promotes β-cell proliferation, both in vitro and in vivo in mice. Irisin can also restore the functional defects characteristic of islets from T2D patients. Although it has been demonstrated that irisin mediates its effects on bone and adipose tissue via αV integrin receptors, the presence of an irisin receptor in β-cells has not been reported.

In INS-1E rat insulinoma cells, we found that irisin activates its intracellular signalling and enhances GSIS in the presence of a specific αV integrin knockdown or a chemical inhibitor of cellular integrins (RGDS), thus excluding the involvement of integrin receptors in irisin effects. In addition, irisin was not able to activate focal adhesion kinase (FAK) which is the main intracellular mediator of integrins-activated signalling. Through a pull-down assay/mass

spectrometry approach, we identified 102 irisin interactors in human pancreatic islets, mostly belonging to intracellular compartments, and not including canonical membrane receptors. We therefore hypothesized that irisin could be endocytosed in pancreatic β-cells and confirmed this by immunoblot analysis of intracellular proteins and immunofluorescence assay. Moreover, both nystatin, an inhibitor of lipid-raft dependent endocytosis, and heat-induced irisin denaturation reduced irisin entry into β-cells. Finally, to investigate the role of endocytosis in irisin biological effects, we used an his-tag irisin that is not endocytosed. In this condition, we found that his-tag irisin was not able to increase GSIS but still enhanced insulin content in INS-1E cells.

These results suggest that irisin effects on pancreatic β-cells are independent of engaging the αV integrin receptor. To date, we found that irisin may not recognize canonical membrane receptors and is instead endocytosed in INS-1E cells. Further studies will be necessary to clarify the role of endocytosis in irisin biological effects, confirming the data obtained also in human and murine islets.

- **9th Spring Meeting, Rimini, February 25-27, 2024**

Identification of myokine irisin receptor in pancreatic beta-cells

Martina Rella [1], Nicola Marrano[1], Anna Borrelli[1], Giuseppina Biondi[1], Angelo Cignarelli[1], Sebastio Perrini[1], Luigi Laviola[1], Francesco Giorgino[1], and Annalisa Natalicchio[1].

[1]Department of Precision and Regenerative Medicine and Ionian Area, Section of Internal Medicine, Endocrinology, Andrology and Metabolic Diseases, University of Bari Aldo Moro, Bari, Italy.

Aim: Irisin, a hormone secreted by skeletal muscle, is able to protects human and rodent beta-cells and pancreatic islets from lipotoxicity-induced apoptosis, to increase insulin biosynthesis and glucose-stimulated insulin secretion (GSIS), and to promote beta-cell proliferation, both in vitro and in vivo in mice. Although it has been demonstrated that irisin mediates its effects on bone and fat via αV integrin receptors, the presence of an irisin receptor in pancreatic beta-cells has not been reported.

Methods: INS-1E rat insulinoma cells were treated with 30 nM αV integrin siRNA for 24 h or 1 μM RGDS (a chemical inhibitor of cellular integrins) for 10 min, and then exposed to 100 nM irisin for different times. Intracellular signalling and GSIS were evaluated by

immunoblotting and insulin ELISA assay, respectively. In human pancreatic islets, irisin interactome was assessed through a pull-down assay/mass spectrometry approach.

Results: In INS-1E cells, irisin activates its intracellular signalling and enhances GSIS in the presence of αV integrin knockdown or RGDS, thus excluding the involvement of integrin receptors in these effects. In human pancreatic islets, we identified 102 irisin interactors, mostly belonging to intracellular compartments (i.e., vesicles and membrane rafts), and not including canonical membrane receptors. We therefore hypothesized that irisin could be endocytosed in pancreatic beta-cells and confirmed this by immunoblotting and immunofluorescence techniques in INS-1E cells.

Conclusions: These results suggest that irisin effects on pancreatic beta-cells are independent of engaging the αV integrin receptor and may instead depend on its endocytosis, thus proposing a potential new mechanism of action for peptide hormones. In addition, we highlight the possibility that the same hormone may signal through different receptors in different target tissues. These findings pave the way for the development of a new class of anti-diabetes drugs.

Abstracts Presented at National and International Scientific Conferences (Co-author)

- **85th ADA congress, June 20-23, 2025, Chicago**

Specific silencing of pancreatic β-cell p66Shc using microfluidic-produced RNA-delivering lipid nanoparticle to prevent the onset and progression of type 2 diabetes. Giuseppina Biondi[1], Nicola Marrano[1], **Martina Rella**[1], Valerio Galasso[1], Giovanni Galluzzi[1], Angelo Cignarelli[1], Sebastio Perrini[1], Luigi Laviola[1], Francesco Giorgino[1], and Annalisa Natalicchio[1]

- **60th EASD Annual Meeting, September 9-13, 2024, Madrid**

Irisin restores the secretory function of pancreatic beta-cells in experimental and human type 2 diabetes. Marrano, N.; Borrelli,A.; Biondi, G.; **Rella, M**; Roberto, L.; Vincenti,L; Cignarelli, A.; Perrini, S.; Laviola, L; Giorgino, F; Natalicchio, A. Short Oral Discussion.

- **59th EASD Annual Meeting, October 2-6, 2023, Hamburg**

The myokine irisin is endocytosed and signals through an αV integrin-independent mechanism in pancreatic beta-cells. Marrano, N.; Borrelli, A.; **Rella, M**; Biondi, G.;Cignarelli, A.; Perrini, S.; Laviola, L.; Giorgino, F.; Natalicchio, A. Short Oral Discussion.

- **83rd ADA congress, June 23-26, 2023 San Diego**

The Myokine Irisin is Endocytosed and Signals Through an αV Integrin-Independent Mechanism in Pancreatic β-cells

Marrano, N.; Borrelli, A.; **Rella, M**; Biondi, G.;Cignarelli, A.; Perrini, S.; Laviola, L.; Giorgino, F.; Natalicchio, A.

- **58th EASD Annual Meeting, September 19-23, 2022. Stockholm & Online. Diabetologia**

Irisin administration restores beta-cell functional mass in a mouse model of type 2 diabetes. Marrano, N.; Biondi, G.; Borrelli, A.; **Rella, M.**; Roberto, L.; Cignarelli, A.; Perrini,S.; Laviola, L.; Giorgino, F.; Natalicchio, A. Oral Presentation.

- **30th SID National Congress, Rimini, 23–26 October 2024**

GLP-1 receptor agonists prevent the apoptosis and dysfunction induced by pasireotide in beta-cells. Biondi, G.; Marrano, N.; Borrelli, A.; **Rella, M**.; Vincenti, L.; Cignarelli, A.; Perrini, S.; Laviola, L.; Giorgino, F.; Natalicchio, A. Oral presentation.

- **30th SID National Congress, Rimini, 23–26 October 2024**

Irisin restores the secretory function of pancreatic beta-cells in experimental and human T2D. Borrelli, A.; Marrano, N.; Biondi, G.; **Rella, M.**; Roberto, L.; Vincenti, L.; Baruzzi, F.; Marchetti, P.; Piemonti, L.; Cignarelli, A.; Perrini, S.; Laviola, L.; Giorgino, F.; Natalicchio, A. Oral presentation,

- **42nd SIE National Congress, Rome, 28 June – 1 July 2023**

Irisin administration restores beta-cell functional mass in a mouse model of type 2 diabetes. Borrelli, A.; Marrano, N.; Biondi, G.; **Rella, M.**; Roberto, L.; Cignarelli, A.; Perrini, S.; Laviola, L.; Giorgino, F.; Natalicchio, A. Oral presentation.

- **42nd SIE National Congress, Rome, 28 June – 1 July 2023**

The myokine irisin is endocytosed and signals through an aV integrin-independent mechanism in pancreatic beta-cells. Marrano, N.; Borrelli, A.; **Rella, M.**; Biondi, G.; Cignarelli, A.; Perrini, S.; Laviola, L.; Giorgino, F.; Natalicchio, A. Oral presentation.

- **29th SID National Congress, Rimini, 26–29 October 2022**

I farmaci incretinici contrastano il danno indotto da pasireotide in beta-cellule pancreatiche. Biondi, G.; Marrano, N.; Borrelli, A.; **Rella, M.**; Vincenti, L; Cignarelli, A.; Perrini, S.; Laviola, L.; Giorgino, F.; Natalicchio, A. Poster.

- **29th SID National Congress, Rimini, 26–29 October 2022**

L'irisina ripristina la massa funzionale beta-cellulare e l'omeostasi glicemica in topi diabetici. Borrelli, A.; Marrano, N.; Biondi, G.; **Rella, M.**; Roberto, L.; Cignarelli, A.; Perrini, S.; Laviola, L.; Giorgino, F.; Natalicchio, A. Oral presentation.

- **29th SID National Congress, Rimini, 26–29 October 2022**

Effetto delle terapie anti-diabete sulla secrezione di irisina in pazienti con diabete di tipo 2. Marrano, N.; Biondi, G.; Le Grazie, G.; Montedoro, A.; Di Gioia, L.; Guarini, F.; Borrelli, A.; **Rella, M.**; Cignarelli, A.; Perrini, S.; Laviola, L.; Giorgino, F.; Natalicchio, A. Poster discussion,

Scientific Publications

- ***Adipose Tissue Secretion Pattern Influences β-Cell Wellness in the Transition from Obesity to Type 2 Diabetes.*** Biondi, G.; Marrano, N.; Borrelli, A.; **Rella, M.**; Palma, G.; Calderoni, I.; Siciliano, E.; Lops, P.; Giorgino, F.; Natalicchio, A. Int. J. Mol. Sci. 2022, 23, 5522. https://doi.org/10.3390/ijms23105522. International Journal of Molecular Science 2022.

- ***The p66Shc protein mediates insulin resistance and secretory dysfunction in pancreatic beta-cells under lipotoxic conditions.*** Biondi, G.; Marrano, N.; Dipaola, L.; Borrelli, A.; **Rella, M.**; D'Oria, R.; Genchi, V. A.; Caccioppoli, C.; Porreca, I.; Cignarelli, A.; Perrini, S.; Marchetti, P.; Vincenti, L.; Laviola, L.; Giorgino, F.; Natalicchio, A. https://doi.org/10.2337/db21-1066. Diabetes 2022.

- ***Type 2 Diabetes and Alzheimer's Disease: The Emerging Role of Cellular Lipotoxicity.*** Marrano, N., Biondi, G., Borrelli, A., **Rella, M.**, Zambetta, T., Di Gioia, L., Caporusso, M., Logroscino, G., Perrini, S., Giorgino, F., & Natalicchio, A. (2023). Biomolecules, 13(1), 183. https://doi.org/10.3390/biom13010183

- ***The Myokine Irisin Ameliorates the Secretory Dysfunction of Pancreatic β-Cells in Experimental and Human Type 2 Diabetes.*** Marrano, N.; Borrelli, A.; Biondi, G.; **Rella, M.**; D'Oria, R.; Genchi, V. A.; Caccioppoli, C.; Galasso, V.; Galluzzi, G.; Roberto, L.; Signorile, A.; Vincenti, L.; Aquilino, F.; Nano, R.; Baruzzi, F.; Moretti, A.; Lupo, L. G.; Marchetti, P.; Piemonti, L.; Cignarelli, A.; Perrini, S.; Laviola, L.; Giorgino, F.; Natalicchio. Currently under revision for Science Advances (2025).

Table of contents

Abstract

Type 2 diabetes (T2D) is characterized by a progressive loss of pancreatic β-cell functional mass, highlighting the need for therapeutic strategies that preserve insulin secretory capacity. Irisin, a myokine induced by physical activity and nutritional cues, has been shown to promote β-cell survival and glucose-stimulated insulin secretion (GSIS); however, the molecular mechanisms underlying its action in pancreatic β-cells remain poorly defined.

Here, we investigated the upstream signaling mechanisms mediating irisin action in pancreatic β-cells. Although integrin αV/β5 has been identified as a functional irisin receptor in other tissues, we demonstrate that irisin signaling in pancreatic β-cells is integrin-independent. Irisin failed to activate focal adhesion kinase (FAK), and inhibition or silencing of integrin αV did not impair irisin-induced AKT and CREB activation or its insulinotropic effect.

Proteomic and in silico analyses suggested the involvement of intracellular compartments associated with endocytic trafficking. Consistently, we show that irisin undergoes cellular internalization in pancreatic β-cells through a lipid raft-dependent mechanism. Disruption of this pathway markedly reduced irisin uptake, while His-tagged irisin, which is not endocytosed, failed to stimulate insulin secretion, indicating that endocytosis is required for its biological activity. Ligand-receptor capture TriCEPS (LRC-TriCEPS) preliminary experiments further demonstrated that irisin binds the β-cell plasma membrane prior to internalization. Moreover, using LRC-TriCEPS coupled with quantitative mass spectrometry, we identified a restricted set of plasma membrane-associated proteins specifically enriched in irisin-treated samples, including F1M9V7, EPDR1, SCRB1 and LYPA1, suggesting potential candidate components involved in irisin binding and uptake.

These results provide a starting point for future studies aimed at defining the molecular machinery underlying irisin internalization and signaling, with potential implications for the development of novel strategies to preserve β-cell function in T2D.

1. Introduction

1.1 Pathogenetic mechanisms in type 2 diabetes (T2D): the role of β-cell functional mass

The latest International Diabetes Federation (IDF) Diabetes Atlas reports that 11.1%, or 1 in 9, of the adult population (20–79 years) is living with diabetes, with over 4 in 10 unaware that they have the condition. By 2050, it has been estimated that 1 in 8 adults (approximately 853 million people) will be living with diabetes, representing a 46% increase (1).

The conventional clinical classification of diabetes includes four categories:
• **Type 1 diabetes (T1D)** (due to autoimmune β-cell destruction, usually leading to absolute insulin deficiency, including latent autoimmune diabetes in adults);
• **Type 2 diabetes (T2D)** (due to a nonautoimmune progressive loss of adequate β-cell insulin secretion, frequently on the background of insulin resistance);
• **Specific types of diabetes due to other causes**, e.g., monogenic diabetes syndromes, diseases of the exocrine pancreas, and drug- or chemical-induced diabetes;
• **Gestational diabetes mellitus**, i.e., diabetes diagnosed in the second or third trimester of pregnancy that was not clearly overt diabetes prior to gestation (or other types of diabetes occurring throughout pregnancy, such as T1D).

T1D and T2D are heterogeneous diseases, and their clinical signs and disease progression may vary considerably. A progressive loss of β-cell mass and/or function, driven by genetic and environmental factors, is common to both conditions and manifests clinically as hyperglycemia. Once hyperglycemia occurs, individuals are at risk of developing similar chronic complications, although rates of progression may differ. Importantly, T2D is not only a domain of older people; in recent years, a two- to three-fold increase in the incidence of T2D has been noted in younger individuals (<40 years) (2,3).

Classification is important for determining personalized therapy, yet some individuals cannot be clearly classified as having T1D or T2D at diagnosis. In this context, the future identification of individualized therapies will be informed

by improved characterization of the multiple paths leading to β-cell demise or dysfunction.

Age, obesity, and lack of physical activity increase the risk of developing T2D. It occurs more frequently in individuals with prediabetes, prior gestational diabetes mellitus, or polycystic ovary syndrome, as well as in those with hypertension or dyslipidemia and in certain racial, ethnic, and ancestral subgroups. Moreover, T2D is often associated with a strong genetic predisposition or family history in first-degree relatives, and the gut microbiome composition may also affect the likelihood of developing T2D. According to the World Health Organization (WHO), T2D and obesity are becoming an alarmingly serious global health problem (4).

T2D accounts for 90–95% of all diabetes and encompasses individuals who generally have relative (rather than absolute) insulin deficiency and insulin resistance (IR), defined as decreased biological responses to insulin. Patients with T2D are generally obese or overweight. Obesity is strongly associated with T2D through pathways regulated by the central nervous system, which controls food intake and energy expenditure by integrating signals from peripheral organs and the environment; excess weight itself contributes to IR (2,3).

Accordingly, T2D is characterized by variable degrees of β-cell dysfunction and IR (5). β-cell dysfunction leads to impaired insulin secretion and an inability to maintain physiological glucose levels, while IR promotes hepatic glucose production and decreases glucose uptake in muscle, liver, and adipose tissue, creating a flawed feedback loop between insulin action and secretion that drives hyperglycemia (2).

Obesity is recognized as a major determinant of β-cell loss and dysfunction. β-cell failure progresses through three sequential phases: 1. compensatory β-cell hyperplasia associated with insulin hypersecretion; 2. impairment of insulin secretory function; 3. eventual loss of β-cell mass (6). Therefore, loss of β-cell mass may result from β-cell exhaustion due to prolonged elevations in glucose

metabolism and insulin secretion, as well as β-cell apoptosis induced by glucotoxicity and lipotoxicity (2).

Transcriptional profiling of β-cells has identified circadian temporal control: during the “active” phase (mealtimes), genes involved in insulin secretion are stimulated, whereas during the “quiescent” phase, genes involved in β-cell growth, repair, and DNA replication are active (7). Therefore, transient β-cell rest during less metabolically active periods might halt β-cell demise and subsequently ameliorate β-cell function and/or promote the survival of remaining endogenous β-cells (8,9).

Early support for the β-cell rest theory came from exogenous insulin administration, which reduces secretory demand and allows replenishment of insulin stores, recovery of glucokinase activity, and alleviation of oxidative stress. In line with this concept, sequential administration of a glucose-dependent insulinotropic polypeptide receptor (GIPR) antagonist to promote β-cell rest, combined with scheduled periods of GLP-1R-induced stimulation during the active phase, has been shown to improve metabolic control in a mouse model of diabetes; however, sustained inhibition of GIPR function may ultimately lead to negative effects in other tissues such as bone and brain (7).

Similarly, a combination therapy approach has been used to rest β-cells and restore function in db/db mice with impaired β-cell compensation, showing benefits through sequential inhibition of GIPR signaling during the light cycle and activation of GLP-1 receptor signaling during the dark cycle over a 4-week course of treatment (9).

Nevertheless, attenuating metabolic demand to improve β-cell function has not been examined in detail at the level of the β-cell using current T2D therapeutic approaches (8).

Conversely, impaired β-cell function may also result from more complex mechanisms. One proposed mechanism is β-cell dedifferentiation, defined as loss of β-cell identity and β-cell–defining transcription factors, which can occur

as a result of glucotoxicity. Guo et al. showed that β-cells from mouse T2D models and subjects with T2D exhibit reduced expression of mature β-cell transcription factors such as Pdx1 and MafA; moreover, MafA inactivation is associated with impaired glucose-stimulated insulin secretion (GSIS) (3).

Another mechanism is transdifferentiation, i.e., conversion of one terminally differentiated cell type into another. Gao et al. reported that loss of Pdx1 in β-cells leads to acquisition of α-cell physiological features, while Cinti et al. found that β-cells in humans with T2D become dedifferentiated and convert to α- and δ-like cells. Although additional human studies are needed, identifying mechanisms that trigger loss of human β-cell identity may propose new strategies to prevent and delay T2D progression (3).

β-cell function may also be impaired through induction of "disallowed" genes that are upregulated under metabolic stress (such as T2D), while proper β-cell markers are downregulated. Several genes have been proposed as disallowed genes, including repressor element 1 silencing transcription factor (REST), whose repression is necessary for physiological insulin secretion. REST overexpression has been associated with reduced functional β-cell mass and diabetes. Moreover, upregulation of REST leads to activation of dual-specificity tyrosine-regulated kinase 1A (DYRK1A), a kinase involved in repression of β-cell proliferation, contributing to impaired β-cell compensation in T2D. Further studies are needed to clarify disallowed gene regulation in β-cells; histone modifications, DNA methylation, and microRNAs have been proposed as contributing mechanisms. Today, numerous effective medications are available for T2D, alongside non-pharmacological treatments including physical activity, balanced diet, and behavioral/psychological interventions (3).

A major advancement in T2D therapy has been the introduction of glucagon-like peptide-1 receptor agonists (GLP-1RAs), which exert potent glucose-lowering and weight-reducing effects and also show cardioprotective, neuroprotective, and anti-inflammatory actions. Despite clinical efficacy, GLP-1RAs can cause dose-dependent gastrointestinal side effects that may limit tolerability in some

patients. Overall, the chronic and progressive nature of T2D is characterized by gradual decline in β-cell function, which drives worsening glycemic control and establishes a self-perpetuating cycle of β-cell dysfunction. Most currently available anti-diabetic therapies mainly focus on reducing hyperglycemia and improving insulin sensitivity and therefore act largely as symptomatic rather than disease-modifying treatments. Consequently, there is a need for strategies capable of preserving β-cell functional mass and preventing its progressive loss. An ideal anti-diabetic therapy should not only ameliorate hyperglycemia and reduce glucotoxicity, but also halt β-cell decline and promote restoration of functional β-cell mass, ensuring long-term glycemic stability and potentially preventing the onset and progression of T2D (7,10).

1.2 Irisin and its pleiotropic effects

Irisin is a 112-amino acid hormone (~12 kDa) generated by proteolytic cleavage of the extracellular, N-terminal portion of fibronectin type III domain-containing protein 5 (FNDC5) (11,12). FNDC5 contains an endoplasmic reticulum signal peptide, a hydrophobic transmembrane domain, a fibronectin III domain (which largely corresponds to extracellular irisin), and a C-terminal cytoplasmic domain. After N-glycosylation at two potential sites (Asn36 and Asn81 in mouse; Asn7 and Asn52 in human) and cleavage likely mediated by disintegrin and metallopeptidase domain (ADAM) family proteins (e.g., ADAM10), irisin is released into the circulation. Most studies report significantly lower circulating irisin levels in T2D patients than in normoglycemic individuals; however, a meta-analysis including 1,005 patients with obesity and 1,242 controls reported higher circulating irisin levels in people with obesity, a controversial finding that has been interpreted as “irisin resistance,” potentially reflecting increased FNDC5/irisin expression in white adipose tissue (WAT) and reduced expression in skeletal muscle and other tissues (13).

Irisin is mainly secreted in response to physical activity, with levels varying according to exercise intensity, type, duration, and frequency. A meta-analysis reported an ~15% increase in irisin immediately following an acute bout of

exercise. However, uncertainty remains regarding the reliability of current methods to quantify circulating irisin. Although Jedrychowski et al. quantified circulating irisin by tandem mass spectrometry, currently available ELISA assays still show substantial variability and limited accuracy. In addition to physical activity, irisin secretion may be influenced by nutritional composition. We previously demonstrated that a high-fat diet (HFD; 60% energy from fat) rapidly and persistently increases circulating irisin levels in healthy wild-type mice; notably, irisin release from myotubes is stimulated by saturated, but not monounsaturated fatty acids (11).

We have previously demonstrated that irisin may act as both a pancreatic β-cell secretagogue and a survival factor, potentially contributing to skeletal-muscle β-cell crosstalk. Recombinant irisin protects human and rodent β-cells and pancreatic islets from saturated fatty acid-induced apoptosis by enhancing AKT/Bcl-2 signaling. Irisin also promotes proinsulin mRNA transcription and increases insulin content and secretion via a PKA/CREB-dependent mechanism, as shown by the ability of the PKA inhibitor H-89 to abolish these effects. Moreover, irisin promotes β-cell proliferation through ERK1/2 activation. In vivo, irisin improved GSIS and increased insulin content and β-cell mass and proliferation in healthy wild-type mice, while only slightly reducing α-cell mass (11,12).

Beyond pancreatic effects, irisin promotes energy expenditure and contributes to glucose homeostasis (11) (**Fig.1**). Exercise-induced FNDC5/irisin upregulation promotes browning of WAT by increasing expression of thermogenic genes (e.g., Prdm16, Dio2, Cox-7a, PGC-1α, UCP-1). Activated beige fat dissipates energy as heat by absorbing excess substrates (fatty acids and glucose), thereby improving obesity and T2D features (13). Consistently, irisin administration improves glycemic control and promotes weight loss in diabetic and/or obese models, supporting its pleiotropic role in energy metabolism across multiple tissues and pathways (11).

Irisin acts as an anti-obesity and anti-diabetic factor via regulating glucose and cholesterol synthesis metabolism in the liver, the main site of gluconeogenesis and glycogenesis. Irisin can enhance liver glycogen synthesis by activating PI3K/AKT/GSK3-GS pathway and inhibit gluconeogenesis via activating AMPK-PEPCK/G6Pase as well as PI3K/AKT/FoxO1-PEPCK and G6Pase pathway. In addition, irisin alleviates inflammation and oxidative stress in liver injury induced by Ischemia-Reperfusion (I/R) (13).

Interestingly, recent evidence suggests that irisin plays a developmental role in regulating neuronal differentiation and maturation, induces the expression of neurotrophic factors such as brain-derived neurotrophic factor (BDNF), and could exert neuroprotective effects in neurodegenerative diseases by improving memory impairment and synaptic plasticity (13,14). Moreover, irisin ameliorates learning and memory function, regulates cognitive function, promotes neurogenesis, and prevents neuronal damage caused by oxidative stress, thus representing a potential target for Alzheimer Disease (AD) treatment and for preventing AD onset. Of note, irisin levels are reduced in both the serum of T2D patients and the cerebrospinal fluid of AD patients (14). Concordantly, Lourenco et al. showed that FNDC5/irisin expression was reduced in the hippocampi and cerebrospinal fluid of AD models, resulting in impaired synaptic plasticity and memory (13).

The concentration of FNDC5/irisin is known to be strongly correlated with bone mineral density (BMD) and bone homeostasis. A cross-sectional and case-control study showed that low concentrations of irisin in serum were related to hip fractures and osteoporosis in postmenopausal women. FNDC5/irisin deletion in osteoblast lineage resulted in a lower bone density and delayed bone development and mineralization in mice. Consistently, systemic FNDC5 Knockout (KO) mice resulted in low bone strength and mass than Wild type (WT) mice, and global FNDC5/irisin KO also completely blocked OVX-induced osteocytic osteolysis and trabecular bone loss (13).

During physical activity and skeletal muscle contraction, the Ca^{2+} level is increased significantly in the cytoplasm of muscle cells and then stimulates the phosphorylation of AMPK, which, in turn, enhances PGC-1α and regulates transcription of downstream factors such as FNDC5. Therefore, AMPK–PGC-1α (PPARγ coactivator-1α)-FNDC5 axis is the most important pathway for irisin synthesis (13).

The blood circulation level of irisin has been identified as a biomarker for muscle mass and performance. Circulating irisin levels in patients with sarcopenia and pre-sarcopenia were lower compared with that in non-sarcopenic participants. Exposure to an ambient hypoxic environment can cause skeletal muscle loss and atrophy, along with the low concentration of irisin in blood circulation both in humans and mice, which could be one of the reasons of muscle atrophy induced by hypoxia. Finally, irisin plays key regulatory role in muscle growth and differentiation by activating downstream ERK1/2 and IL-6 pathways in myoblasts, in an autocrine manner (13).

Cardiovascular diseases (CVDs) include hypertension, coronary artery disease, myocardial infarction, heart failure, atherosclerosis, and myocardial I/R injury, which are the leading cause of human death worldwide. Irisin may play a crucial role, since regular exercise can reduce the risk of CVDs. It has been demonstrated that patients with CVDs exhibited significantly lower serum irisin levels than that in healthy people. Li et al. revealed that resistance exercise could activate irisin release from skeletal muscle and then stimulate the AMPK-PINK1/Parkin-LC3/P62 signaling pathway, which regulated mitophagy and inhibited oxidative stress in the myocardium (13).

Irisin has been inversely associated with kidney injury and could serve as a diagnostic biomarker for kidney diseases. A systematic review and meta-analysis of 9 studies on 859 Chronic Kindey Disease (CKD) patients and 393 non-CKD individuals confirmed that irisin levels were significantly downregulated in CKD patients than in the healthy controls. The subgroup analysis also found that hemodialysis (HD) and peritoneal dialysis (PD) patients had reduced irisin levels

relative to non-dialysis CKD patients. Further, it has been suggested that median irisin levels (corrected for age, sex, and BMI) decreased progressively with CKD progression. Moreover, several studies have found a direct association between GFR and irisin levels, which further validate that irisin could be used as an early predictor and diagnostic marker of renal function in kidney diseases (15).

In addition to these correlational studies, mechanistically, irisin may have beneficial effects directly within the kidney, improving kidney function through enhancing the oxidative capacity of renal tubular cells and reducing renal fibrosis via the TGFβ/Smad 2 pathway (16).

Figure 1. Irisin and its pleiotropic effects

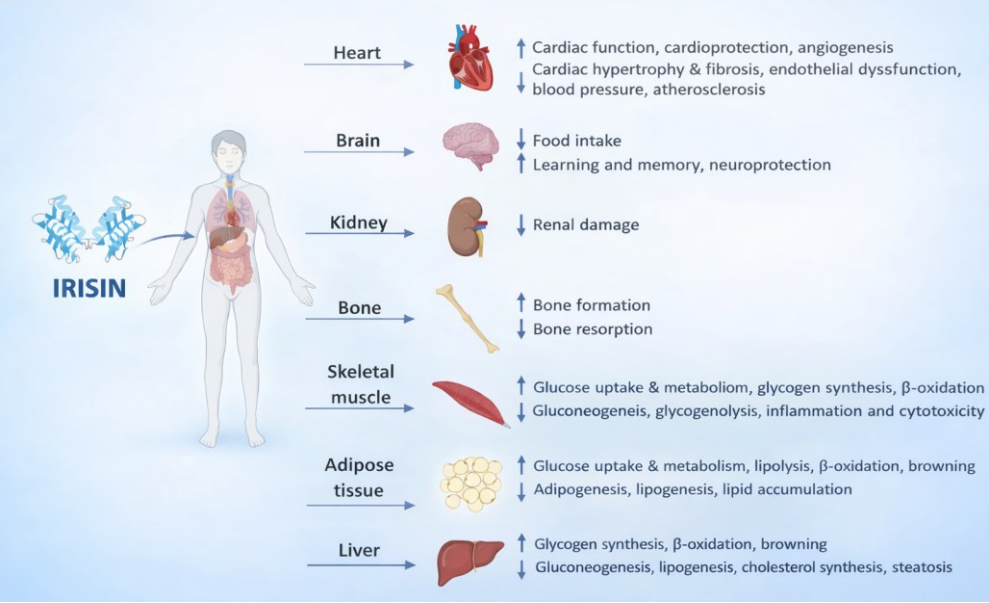

Fig. 1. Irisin and its pleiotropic effects. Schematic representation of the pleiotropic effects of irisin on different target tissues. Irisin exerts beneficial metabolic and protective actions in multiple organs, including heart, brain, kidney, bone, skeletal muscle, adipose tissue, and liver, where it modulates glucose and lipid metabolism, energy expenditure, tissue homeostasis, and stress responses. Upward and downward arrows indicate processes that are positively or negatively regulated by irisin, respectively.

1.3 Irisin receptor in other tissues

In bone, adipose tissue, and hippocampus, irisin appears to signal primarily through αV integrin receptors, particularly αV/β5. Kim et al. demonstrated, through a combination of biochemical and functional approaches, that irisin

exerts its effects in bone and adipose tissue by signaling through the αV/β5 integrin (17,18).

Specifically, protein-protein binding assays using purified irisin and integrin complexes showed that irisin displays the highest apparent affinity for αV/β5 in osteocyte cells. Furthermore, hydrogen-deuterium exchange mass spectrometry (HDX/MS) enabled the mapping of binding motifs on both irisin and the integrin complex. In bone tissue, irisin stimulation resulted in focal adhesion kinase (FAK) phosphorylation, the main intracellular mediator of integrin signaling, while cellular integrin inhibition or the use of antagonistic antibodies directed against αV/β5 suppressed nearly all irisin-mediated signaling and downstream gene expression (17).

Kim et al. also provided evidence that irisin may exploit extracellular Hsp90α, a stress-induced factor, to mediate integrin activation (18). However, whether a relatively small protein such as irisin can efficiently interact with and signal through integrins remains mechanistically complex, as integrin-ligand interactions with their canonical partners, typically large extracellular matrix proteins, are usually highly structured and multivalent.

αV integrins belong to the integrin family lacking the inserted αI domain and classically recognize ligands containing the Arg-Gly-Asp (RGD) motif. For most fibronectin type III (FNIII) domain-containing ligands, the RGD sequence is presented in a flexible loop that forms a small interaction interface with both the α and β integrin subunit heads. Notably, irisin consists of a single FNIII domain and lacks an RGD motif. Moreover, irisin is substantially smaller than canonical integrin ligands and circulates at much lower concentrations. These structural features raise important questions regarding how irisin can activate integrins and whether this process requires cofactors such as Hsp90α, with definitive clarification likely requiring atomic-level structural resolution (18).

It is generally assumed that the circulating and biologically active form of irisin exists predominantly as a dimer, with an apparent molecular weight of

approximately 39-48 kDa. Crystallographic analyses revealed that irisin adopts a stable dimeric structure characterized by an antiparallel β-sheet interface stabilized by multiple hydrogen bonds between the monomers (19).

Based on these structural data, it has been proposed that irisin may function as a preformed dimeric ligand or act as a paracrine or autocrine dimerization module in the context of full-length FNDC5-like receptors, potentially enabling signal initiation through receptor clustering (20). However, an integrin-based receptor model may not readily accommodate the dimeric structure of irisin. The irisin dimer has an estimated width of approximately 40 Å, whereas the head domain of a single integrin measures about 47 Å, suggesting that a dimeric irisin molecule would be expected to engage only one integrin at a time rather than promoting integrin clustering. This consideration would be less relevant if circulating irisin were predominantly monomeric at nanomolar concentrations; however, available crystal structures strongly support a stable dimeric configuration, although the dissociation constant for dimer formation has not yet been experimentally determined (21). To provide a mechanistic explanation for these observations, Kim et al. proposed a two-step mechanism involving extracellular Hsp90α. Docking models based on biochemical assays and biophysical HDX-MS data revealed a distinct integrin-ligand binding mode in which irisin adopts a broad, “pancake-like” conformation and primarily engages the β5 integrin subunit at a site clearly distinct from the classical RGD-binding site. Multiple atomic interactions stabilize this configuration, providing high-affinity binding and enabling a global conformational rearrangement of the integrin subunits sufficient to elicit signal transduction. However, how the downstream signaling generated by this non-canonical binding mode differs from that induced by RGD-containing ligands remains to be determined (18).

Importantly, the identification of integrin αV/β5 as the primary irisin receptor in osteoblasts does not exclude the possibility that other, yet unidentified receptors mediate irisin effects in different tissues (22–24).

In a translational model of pulmonary I/R injury, irisin administration exerted marked cytoprotective effects, including preservation of mitochondrial integrity and attenuation of oxidative stress and apoptosis-related pathways. Mechanistically, irisin was shown to undergo cellular internalization, as evidenced by its intracellular accumulation following extracellular administration. Pharmacological inhibition of lipid raft-dependent endocytosis using nystatin markedly reduced irisin uptake and abrogated its protective effects, indicating that irisin internalization occurs predominantly via a cholesterol-dependent, caveolae-mediated endocytic pathway. (25).

Consistent with this notion, previous studies have reported membrane binding of irisin in cardiomyoblasts and preadipocytes, supporting the presence of cell-surface binding partners for irisin across different cell types, although their molecular identity remains unclear (26).

In the liver, irisin has been shown to modulate inflammatory signaling through interaction with the MD-2 component of the MD-2/TLR4 complex. In models of non-alcoholic fatty liver disease, irisin competitively binds MD-2, preventing MD-2/TLR4 complex formation and subsequent TLR4-dependent activation of pro-inflammatory signaling pathways, including NF-κB, thereby ameliorating metabolic dysfunction (27). Beyond integrins, TRPC3 has been proposed as a functional irisin receptor in adipose-derived mesenchymal stem cells. TRPC3 is a plasma membrane-localized, non-selective cation channel belonging to the TRPC family and mediates receptor-operated Ca^{2+} entry in response to extracellular stimuli. In this cellular context, irisin was shown to physically interact with TRPC3, as demonstrated by co-immunoprecipitation and biophysical binding assays. This interaction induces a rapid Ca^{2+} influx and activation of downstream Ca^{2+}-dependent signaling pathways, including AKT and ERK. Pharmacological inhibition or genetic ablation of TRPC3 abolishes irisin-induced Ca^{2+} entry, downstream signaling activation, and the associated transcriptional responses, indicating that TRPC3 is required for irisin signaling in adipose-derived mesenchymal stem cells. Collectively, these findings support

the concept that irisin signaling is not universally mediated by integrins but rather relies on distinct, tissue-specific membrane components and mechanisms depending on the cellular context (27).

2. Aim

In T2D patients, β-cell function is already reduced by about 50% at diagnosis and further declines thereafter. β-cell mass is also reduced in subjects with T2D, and islets from diabetic donors are smaller compared to non-diabetic donors. Thus, β-cell regeneration and/or preservation of the functional islet integrity should be highly considered for T2D treatment. To date, the available anti-diabetes drugs have been developed as "symptomatic" medications since they act to primarily reduce elevated blood glucose levels (10). GLP-1RAs are newly approved medications for the treatment of diabetes and obesity. GLP-1 is an intestinal peptide secreted by epithelial L-cells in response to nutrient intake, particularly glucose and lipids. GLP-1 exerts physiological effects on various organs. As an incretin, it enhances glucose-dependent insulin secretion by pancreatic β-cells, promotes β-cell neogenesis, inhibits β-cell apoptosis, and suppresses glucagon secretion from α-cells. Additionally, GLP-1 influences other tissues and organs, including the stomach by delaying gastric emptying, the heart by exerting cardioprotective effects, and adipose tissue and skeletal muscle by improving glucose uptake, and it also acts centrally on neurons in the hypothalamus, inducing a feeling of satiety. Various GLP1-RAs have been authorized for managing T2D and these medications are primarily administered via subcutaneous injection. Long-acting agents within this drug class are associated with more effective glucose lowering and exhibit fewer gastrointestinal side effects compared to their short-acting counterparts. Given that GLP-1 analogs are a relatively new and insufficiently studied class of drugs, their adverse effects are not yet fully understood. However, among the side effects identified so far, nausea and vomiting are the most common. Furthermore, nasopharyngitis and headaches associated with injections may occasionally occur (3). A truly efficient anti-diabetes medication, capable to

prevent the onset and progression of T2D, should stop β-cell loss and/or promote the restoration of fully functional β-cell mass, independently of reducing hyperglycemia and ameliorating glucotoxicity on the pancreatic islets (10). In this context, irisin has emerged as a circulating hormone able to promote β-cell survival and insulin secretion by activating pro-survival (AKT/Bcl-2) and secretory (PKA/CREB) pathways, as well as enhancing β-cell proliferation via ERK1/2 (11).

Irisin can be considered an incretin-like hormone, as its secretion appears to be also affected by meals and, once secreted, it enhances insulin secretion in a glucose-dependent manner. In addition, both the GLP-1 insulinotropic effects and irisin levels are defective in T2D, and their exogenous administration is able to improve glycemic control. Importantly, irisin and GLP-1 share numerous direct pancreatic effects, including the ability to induce insulin biosynthesis and GSIS, as well as improving β-cell proliferation and survival. Albeit through different pathways, irisin and GLP-1 activate the same intracellular signaling proteins (e.g., AKT, CREB, ERK1/2). Interestingly, irisin shows cardiovascular and anorexigenic effects similar to those of GLP-1, while demonstrating a more pronounced beneficial metabolic effect in insulin-dependent organs, such as liver, skeletal muscle, and adipose tissue. Of note, because GLP-1 and irisin signal through different receptors that nevertheless converge on very similar pathways, an additive effect of the two molecules cannot be excluded. This evidence highlights the promising antidiabetic and antiobesity potential of irisin, possibly in combination therapeutic regimens with GLP-1RAs (11). However, the upstream mechanisms mediating irisin action remain incompletely defined and appear to be tissue-dependent. While αV integrins, particularly αV/β5, have been identified as functional receptors in bone and adipose tissue (17,18, 28), additional evidence supports alternative mechanisms, including TRPC3 as a functional binding partner in adipose-derived mesenchymal stem cells (27) and modulation of the MD-2/TLR4 pathway in liver models. Moreover, irisin cellular uptake has been reported in a translational model of pulmonary I/R injury, in which pharmacological inhibition of lipid raft-dependent endocytosis

with nystatin reduced irisin internalization and abolished its protective effects (25).

Collectively, these findings indicate that irisin signaling is not universally mediated by a single receptor system and that the identity of the membrane component(s) responsible for irisin binding, internalization, and signal initiation remains unresolved in pancreatic β-cells. The identification of this mechanism with these characteristics would represent a truly effective antidiabetic therapeutic strategy, as it could prevent the onset and progression of diabetes by blocking β-cell loss and/or promoting the restoration of fully functional β-cell mass (10).

3. Materials and Methods

Cell culture

Immortalized human pancreatic β-cells 1.1B4 (CSC-I2273Z Creative Bioarray) were cultured in a 5% CO2 atmosphere at 37 °C in RPMI 1640 medium containing 11 mmol/l glucose and supplemented with 10% v/v FBS, and 1% v/v penicillin and streptomycin (all from Thermo Fisher Scientific, Waltham, Massachusetts, USA).

Rat insulin-secreting INS-1E cells (RRID:CVCL_0351) were cultured in a 5% CO2 atmosphere at 37 °C in RPMI 1640 medium containing 11 mmol/l glucose and supplemented with 10% v/v heat inactivated FBS, 1% v/v penicillin and streptomycin, 1% v/v non-essential amino acids (all from Thermo Fisher Scientific, Waltham, Massachusetts, USA), 10 mmol/l HEPES pH 7.4, 1 mmol/l pyruvic acid, and 50 μmol/l β-mercaptoethanol (all from Sigma-Aldrich). INS-1E cells were treated with 100 nmol/l irisin (AG-40B-0103 AdipoGen Life Sciences) at the indicated times (selected on the basis of dose-response studies performed in our previous study (12), 1 μmol/l RGDS peptide (R&D Systems Cat. # 3498/10), 30 nmol/l integrin αV siRNA #ITGAV (Catalog #4390771 Thermo Fisher Scientific) (selected on the basis of dose-response studies), 100

nmol/l C-term His-tag irisin (BP152-50ug CliniSciences) at the indicated times, 53 μmol/l nystatin (lipid raft-mediated endocytosis inhibitor, N1638 Sigma-Aldrich), 6 μg/μl TriCEPS, selected on the datasheet instructions (#P05203 DualsystemsBiotech).

Pancreatic islets isolation and culture

Murine islets were isolated from 8 weeks-old male C57Bl/6J mice (purchased from Biogem S.c.a.r.l., Ariano Irpino 83031). Isolation was achieved by collagenase digestion and density gradient purification. Murine islets were cultured free floating at 37 °C in RPMI 1640 culture medium containing 5.5 mmol/l glucose, supplemented with 10% v/v FBS, 1% v/v penicillin and streptomycin, 50 μg/ml gentamicin (all from Thermo Fisher Scientific), and 0.25 μg/ml amphotericin (Aurogene s.r.l., Roma, Italy).

Isolated human islets were obtained from pancreatic biopsies of 2 subjects without diabetes (donor characteristics are reported in **Tab.1**) with the approval of the Ethics Committees of the University Hospital Policlinico of Bari (study approval number: 5316, approved on 637 29/11/2017, with amendments on 17/10/2018 and 17/05/2023). Informed consent was obtained from each donor patient prior to the collection of pancreatic biopsies. Pancreatic biopsies were from patients undergoing duodeno-cefalo pancreatectomy (dpc) for Vater's ampulla tumors at the Division of General Surgery of the Polyclinic Hospital of Bari (Bari, Italy) or at Pisan University Hospital-Unit of Metabolic Diseases and Diabetology, Cisanello Hospital (Pisa, Italy). Isolation was achieved by collagenase digestion and density gradient purification, as previously detailed (12,28). Isolated islets were then cultured free floating at 37 °C in RPMI 1640 culture medium containing 5.5 mmol/l glucose, supplemented with 10% v/v FBS, 1% v/v penicillin and streptomycin, 50 μg/ml gentamicin (all from Thermo Fisher Scientific), and 0.25 μg/ml amphotericin (Aurogene s.r.l., Roma, Italy).

Table 1. Characteristics of pancreatic islets donors

Donor	Source	Isolation Center	Age (yrs)	Sex (M/F)	BMI (kg/m²)	A1C or FG (mg/dl)	Cause of death	Diabetes
1	Human cadaver donor	Pisa	80	F	24.8	91	Cerebral hemorrhage	NO
2	Human cadaver donor	Bari	57	M	20.7	88	Cerebral hemorrhage	NO

Immunoblotting

For protein analysis, INS-1E cells were harvested and homogenized in protein lysis buffer containing 50 mmol/l HEPES pH 7.4, 1% Triton X-100, 150 mmol/l NaCl, 1 mmol/l MgCl2, 1 mmol/l CaCl2, 10% glycerol, 10 mmol/l NaPP, 10 mmol/l NaF, and 4 mmol/l EDTA, supplemented with protease and phosphatase inhibitors (Complete Mini Protease Inhibitor Cocktail Tablets and PhosStop Phosphatase Inhibitor Cocktail Tablets, Roche Diagnostic, Indianapolis, IN, USA). Protein concentration was determined using the Bradford assay (Biorad, Hercules, California, USA). Equal amounts of protein were separated by SDS-PAGE and blotted on polyvinylidene fluoride (PVDF) membranes. Membrane blocking and incubation with primary antibodies were performed with 5% skim milk in Tris-buffered saline (TBS 1X) with Tween, and then membranes were incubated with primary antibodies (a list of the antibodies used is shown in **Tab. 2**) overnight at 4°C, followed by washing with TBS and incubating with a horseradish-peroxidase-conjugated secondary antibody, for 1 h at room temperature. Clarity Western ECL Substrate (Biorad) was used for visualization of proteins with a Model 3000 VersadDoc Imaging System (Biorad). The signal intensity of each protein band was then measured using Quantity One Software (Biorad) and normalized to the corresponding total protein band.

Table 2. Antibodies used for immunoblotting and immunofluoresce assay.

Antibody	Distributor	Source	Dilution
Integrin αV (D2H5F) RRID: AB_2735190	Cell Signaling Technology Inc. #60896	Rabbit monoclonal antibody	1:1000
Irisin	Enzo Life Sciences ENZ-ABS256	Rabbit polyclonal antibody	1:800–1:1000
Phospho-FAK (Tyr397) RRID: AB_2173659	Cell Signaling Technology Inc. #3283	Rabbit monoclonal antibody	1:1000
Total FAK RRID: AB_2269034	Cell Signaling Technology Inc. #3285	Rabbit monoclonal antibody	1:1000
Phospho-AKT (Ser473) RRID: AB_329825	Cell Signaling Technology Inc. #9271S	Rabbit monoclonal antibody	1:1000
Phospho-AKT (Thr308) RRID: AB_329828	Cell Signaling Technology Inc. #9275L	Rabbit monoclonal antibody	1:1000
Total AKT RRID: AB_915783	Cell Signaling Technology Inc. #4691S	Rabbit monoclonal antibody	1:1000
Phospho-CREB (Ser133) RRID: AB_2561044	Cell Signaling Technology Inc. #9198	Rabbit monoclonal antibody	1:1000
Total CREB (48H2) RRID: AB_331277	Cell Signaling Technology Inc. #9197	Rabbit monoclonal antibody	1:1000
β-actin RRID: AB_2714189	Santa Cruz Biotechnology #47778	Mouse monoclonal antibody	1:1000
His-Tag (D10) RRID: AB_2744546	Cell Signaling Technology Inc. #12698	Rabbit monoclonal antibody	1:400–1:1000
Alexa Fluor 488 goat anti-rabbit RRID: AB_143165	Invitrogen A-11008	Secondary antibody	1:500–1:900

Glucose-stimulated insulin secretion (GSIS)

INS-1E cells were seeded into complete medium in 6-well dishes and stimulated with irisin for 1 h; then, they were incubated with low-glucose (3 mmol/l) Krebs-ringer bicarbonate HEPES solution KRBH containing 140 mmol/l NaCl, 3.6 mmol/l KCl, 0.5 mmol/l NaH2PO4, 0.5 mmol/l MgSO4, 1.5 mmol/l CaCl2, 5 mmol/l NaHCO3, 10 mmol/l HEPES, and 0.1% BSA, pH 7.4 with the addition of 100 nmol/l irisin for 1 h. Successively, cells were cultured in low-glucose KRBH for 1 h and then for a further hour in high-glucose KRBH (25 mmol/l). The supernatant fractions were then obtained from each reaction well and frozen at -80 °C for subsequent determination of insulin concentrations. Insulin levels were measured by High Range Rat Insulin ELISA (Mercodia AB; cat. n. 10-1145-01). Cells were harvested and homogenized in non-denaturing lysis buffer containing 50 mmol/l Trizma base, 1% Triton X-100, 150 mmol/l NaCl, and 1 mmol/l EDTA, supplemented with protease and phosphatase inhibitors (Complete Mini Protease Inhibitor Cocktail Tablets and PhosStop Phosphatase Inhibitor Cocktail Tablets, Roche Diagnostic). Insulin secretion was normalized to protein concentration as performed in previous studies (29,30).

Pull-down assay

To identify potential irisin-interacting proteins in pancreatic β-cells, a pull-down assay followed by mass spectrometry (MS) analysis was performed using human pancreatic islet lysates. Briefly, 100 µg of C-terminal His-tagged irisin were immobilized on HisPur™ Cobalt chelate affinity resin (#89966 Thermo Scientific) [(+) irisin], while resin without irisin was used as a negative control [(-) irisin]. Human pancreatic islet protein lysates (800 µL) were incubated with both (+) irisin and (−) irisin resins. As a positive control, HisPur™ Cobalt chelate affinity resin loaded with C-terminal His-tagged irisin but not incubated with pancreatic islet protein lysate was included. After extensive washing, bound proteins were eluted using an imidazole-containing elution buffer. Eluted proteins were precipitated with sodium deoxycholate, trichloroacetic acid, and cold acetone, dried, and resuspended in NuPAGE™ LDS sample buffer

(#NP0008 Thermo Fisher Scientific). Samples were incubated at 65 °C for 20 min, separated by 12% SDS–PAGE, and visualized by Coomassie Blue staining. Protein bands corresponding to the (−) irisin and (+) irisin conditions were subsequently processed for quantitative proteomic analysis (**Fig. 5**).

MS analysis

Protein digestion and peptides purification

Gel lanes coomassie stained were processed according to STAGE-diging protocol (31). Briefly, the entire gel lanes were transferred into the STAGE-diging p1000 tip filled with a double C18 Empore Disk (3M, Minneapolis, MN) plug and submitted to reduction by 10 mmol/l dithiothreitol (DTT), alkylation by 55 mmol/l iodoacetamide (IAA) and finally Trypsin Sequencing Grade, modified from Roche) digestion overnight. Digestion solutions were acidified and desalted passing through the C18 plugs. The eluted peptides were dried in a Speed-Vac and resuspended in solvent A (2% ACN, 0.1% formic acid).

Liquid chromatography-tandem MS (nLC–MS/MS) analysis

4 µl of each digested sample were injected on a UPLC EASY-nLC 1000 (Thermo Scientific) coupled with a quadrupole Orbitrap QExactive-HF mass spectrometer (Thermo Fisher) equipped with a nanoelectrospray ion source (Proxeon Biosystems). Peptides separation was achieved on a linear gradient of 32 min, starting from 95% of solvent A (0.1% formic acid, 2% acetonitrile) and ramping to 50% Solvent B (80% acetonitrile, 0.1% formic acid) in 23 min and from 50% to 100% Solvent B in 2 min at a constant flow rate of 0.25 µl min−1. The nLC system was connected to a 25 cm fused-silica emitter of 75 µm inner diameter (New Objective), packed in house using a high-pressure bomb loader (Proxeon) with ReproSil-Pur C18-AQ 1.9 µm beads (Dr.Maisch). MS data were acquired in data-dependent acquisition mode (DDA), with a top15 method for HCD fragmentation. Survey full scan MS spectra (300–1750 Th) were acquired in the Orbitrap with 60,000 resolution, AGC target 1e6, IT 120 ms. For HCD spectra, the resolution was set to 15,000, AGC target 1e5, IT 120 ms; normalized

collision energy 28%, isolation width 3.0 m/z with a dynamic exclusion of 5 seconds.

Protein identification

For protein identification, raw files were processed using Proteome Discoverer (version 1.4.1.14, Thermo Scientific) and Mascot engine (version 2.6.0, Matrix Science) searching against the Uniprot_cp_Rat downloaded on 10-01-2017 (35838 entries) or Uniprot_cp_HomoSapiens downloaded on 10-01-2017 (156576 entries) database with the following parameters: enzyme Trypsin; maximum missed cleavage 2; fixed modification carbamidomethylation (C); variable modification oxidation (M), protein N-terminal acetylation; peptide tolerance 10 ppm; MS/MS tolerance 20 ppm. Peptide Spectral Matches (PSM) were filtered using percolator based on q-values at a 0.01 False Discovery Rate (FDR) (high confidence). Proteins were considered identified with 2 unique high confident peptides (32).

Scaffold (version Scaffold_4.10.0, Proteome Software Inc., Portland, OR) was used to validate MS/MS based peptide and protein identifications. Peptide identifications were accepted if they could be established at greater than 95,0% probability by the Scaffold Local FDR algorithm. Protein identifications were accepted if they could be established at greater than 99,0% probability and contained at least 2 identified peptides. Protein probabilities were assigned by the Protein Prophet algorithm (33). Proteins that contained similar peptides and could not be differentiated based on MS/MS analysis alone were grouped to satisfy the principles of parsimony. Proteins sharing significant peptide evidence were grouped into clusters.

String database

To predict functional associations among proteins co-eluted with irisin, the STRING database (https://string-db.org/) was queried. Functional enrichment analysis was performed on the resulting protein interaction network. "*Count in network*" indicates the number of proteins within the network annotated with a

given term, relative to the total number of proteins annotated with that term in both the network and the background. "*Strength*" represents the log10 (observed/expected) ratio and reflects the magnitude of enrichment, defined as the ratio between the number of proteins in the network annotated with a specific term and the number expected by chance in a random network of the same size. Statistical significance of enrichment was assessed using the FDR, with p-values corrected for multiple testing within each annotation category using the Benjamini-Hochberg procedure.

Immunofluorescence assay

INS-1E cells were seeded onto glass coverslips in 6-well dishes, cultured in complete medium, and stimulated with 100 nmol/l recombinant irisin or 100 nmol/l His-tagged irisin for different time points. Cells were then fixed with 4% paraformaldehyde for 15 min and permeabilized with TBS containing 0.2% Triton X-100 for 10 min. After this step, cells were incubated overnight at 4 °C with monoclonal primary antibodies directed against recombinant irisin or His-tagged irisin, diluted 1:400 in PBS 1× containing 10% goat serum. On the following day, cells were incubated with an Alexa Fluor 488 goat anti-rabbit secondary antibody (Invitrogen, A-11008) diluted 1:300. Cell nuclei were counterstained with DAPI (Molecular Probes) diluted 1:1000 (a list of the antibodies used is shown in **Tab. 2**). Finally, images were acquired using a Nikon ECLIPSE Ti-S 611 fluorescence microscope (Nikon, Minato, Tokyo, Japan).

Ligand-Receptor Capture TriCEPS™ (LRC-TriCEPS)

Ligand-Receptor Capture TriCEPS (LRC-TriCEPS) is a chemical proteomics technology that enables the identification of cell-surface ligand-receptor interactions and potential off-targets on living cells and tissues through a trifunctional crosslinker. TriCEPS consists of three functional moieties: (i) an NHS-ester group for covalent coupling to primary amines on the ligand of interest, (ii) a protected hydrazone group that covalently captures glycosylated cell-surface target proteins, thereby stabilizing ligand-receptor interactions, and

(iii) a functional handle enabling purification of ligand-receptor complexes prior to MS analysis. During an LRC-TriCEPS experiment, the ligand-TriCEPS conjugate is incubated with living cells expressing unknown targets, while control ligands conjugated to TriCEPS are processed in parallel. Upon incubation, TriCEPS covalently labels cell-surface glycoproteins, including both random surface proteins and ligand-engaged targets; however, proteins specifically interacting with the ligand are more efficiently labeled, allowing their identification by relative quantitative proteomics following enrichment and LC-MS/MS analysis (**Fig.9**).

Before performing the main LRC-TriCEPS experiment, a Flow-TriCEPS pre-test was conducted to assess optimal conditions for ligand binding, including temperature, incubation time, pH, and ligand concentration. In the Flow-TriCEPS configuration, the purification handle of TriCEPS is replaced by a biotin moiety, allowing direct detection of ligand binding by flow cytometry using phycoerythrin (PE)-conjugated streptavidin (**Fig. 8A**).

To perform the pre-test INS-1E cells were seeded in 12-well plates and cultured to approximately 80% confluence. For each experiment, one multi-well plate was prepared and four wells were assigned to different experimental conditions. TriCEPS coupling reactions were performed according to the manufacturer's instructions. Briefly, 20 µg of recombinant irisin, transferrin (positive control), or glycine (negative control) were mixed with 1 µl of TriCEPS reagent in phosphate-buffered saline (PBS) pH 7.4 to a final volume of 50 µl, with TriCEPS added last and gently mixed by pipetting. Coupling reactions were incubated for 40 min at 22 °C under agitation (350 rpm).

For ligand binding, cells were washed once with PBS pH 7.4 and incubated with 200 µl PBS pH 7.4 containing 3 µl of TriCEPS-coupled ligand (final concentration 6 µg/µl) per well. Cells were incubated under the indicated experimental conditions, varying temperature, incubation time, and pH, under gentle agitation and protected from light. After incubation, cells were washed twice with PBS pH 7.4 to remove unbound ligand. For fluorescence labeling,

cells were incubated with PE-conjugated streptavidin (Jackson ImmunoResearch, Code: 016-110-084), diluted 1:50 in PBS (3 µl in 150 µl total volume), for 30 min at 4 °C in the dark. Cells were then washed with PBS pH 7.4, gently detached using a cell scraper in 250 µl PBS pH 7.4, pelleted by centrifugation at 400 × g for 2 min, resuspended in 250 µl PBS pH 7.4, and transferred to flow cytometry tubes for acquisition. Flow cytometry analysis was performed using a Navios EX flow cytometer (Beckman Coulter Life Sciences).

The main LRC-TriCEPS experiment was conducted following the manufacturer's instructions, and using the optimized binding condition (37 °C, 30 min, pH 7.4). Cells were lysed according to standard protocols, and ligand-bound target proteins were purified by solid-phase chromatography. After stringent washing steps to remove nonspecific interactions, proteins were reduced, alkylated, and digested with trypsin. Tryptic peptides were collected and analyzed by LC-MS/MS using an Exploris 480 mass spectrometer (Thermo Fisher Scientific) equipped with an electrospray ion source. Peptides were acquired in data-dependent acquisition mode using a 90-min gradient on a 50-cm C18 packed column.

Mass spectrometry data were processed using FragPipe, integrating MSFragger for peptide identification. Raw files were searched against the UniProt Rat protein database using a target-decoy strategy for FDR estimation. Identifications were filtered to 1% FDR at both peptide and protein levels, and downstream processing, including protein inference and quantification, was performed using Perseus. Relative quantification between ligand and control samples was based on normalized extracted ion intensities. Statistical analysis was performed using a two-sample Student's *t*-test, and results were visualized using volcano plots applying an S-curve threshold that simultaneously accounts for fold change and statistical significance. Proteins exceeding the S-curve threshold were considered significantly regulated and were further filtered for surface-associated proteins based on Gene Ontology (GO) annotation.

Statistical analysis

One-way or two-way ANOVA tests were used for statistical analysis, as appropriate. Tukey's or Sidak's post-hoc analyses were performed as appropriate to identify specific differences. For all statistical tests, a p-value of less than 0.05 was used to identify statistically different values. The used statistical test is indicated in the figure legends for each individual experiment. All values presented are means ± SD.

4. Results

4.1 αV integrin is expressed in pancreatic β-cells

Given that Kim et al. demonstrated that irisin mediates its effects in bone and adipose tissue via the integrin αV receptor (17), we initially assessed whether this integrin is expressed in the endocrine pancreas. Therefore, human and rat cell lines, as well as human and murine pancreatic islets, were lysed and analyzed by immunoblotting to assess the expression of the indicated proteins (**Fig.2**). Immunoblot analysis revealed the expression of integrin αV in rat insulinoma INS-1E cells (lane 1), murine pancreatic islets (lane 2), human pancreatic 1.1B4 cells (lane 3), and human pancreatic islets (lane 4), as evidenced by the presence of a specific band at the expected molecular weight (~140 kDa) in each lane.

Figure 2. αV integrin is expressed in pancreatic β-cells

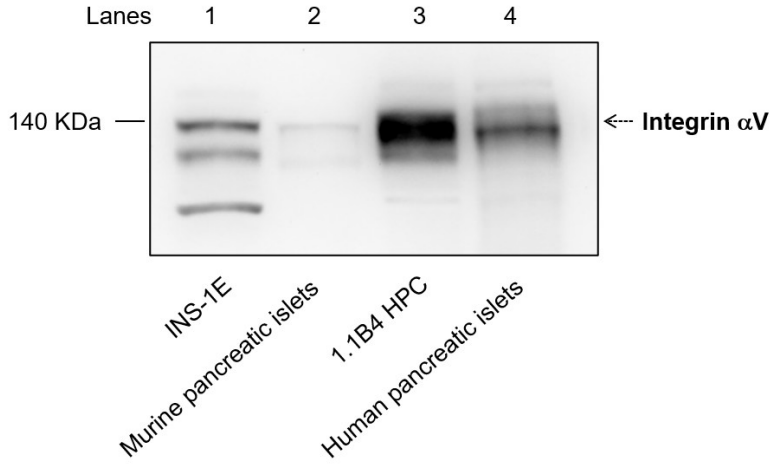

Fig. 2. αV integrin is expressed in pancreatic β-cells. Protein expression of integrin αV was assessed by immunoblotting in rat insulinoma INS-1E cells (lane 1), murine pancreatic islets (lane 2), human pancreatic 1.1B4 cells (lane 3), and human pancreatic islets (lane 4).

4.2 Irisin signals through an integrin-independent mechanism in pancreatic β-cells

We first assessed whether irisin was able to induce phosphorylation of FAK at tyrosine 397 (Y397), the main intracellular mediator of integrin signaling. Subsequently, we examined whether the integrin inhibitor peptide RGDS interfered with the ability of irisin to promote phosphorylation of AKT at threonine 308 (T308) and serine 473 (S473), as well as phosphorylation of CREB at serine 133 (S133) (**Fig. 3A–E**). INS-1E cells were pretreated with 1 μmol/l RGDS and then stimulated with 100 nmol/l irisin for the indicated time points. Immunoblot analysis and relative quantification showed that irisin was unable to activate FAK under any condition tested (**Fig. 3A, B**). Moreover, RGDS did not interfere with irisin-induced phosphorylation of AKT (**Fig. 3A, C, D**) or CREB (**Fig. 3A, E**). Collectively, these preliminary results suggest that irisin may act through a different mechanism in pancreatic β-cells.

Figure 3. Irisin signals through an integrin-independent mechanism in pancreatic β-cells

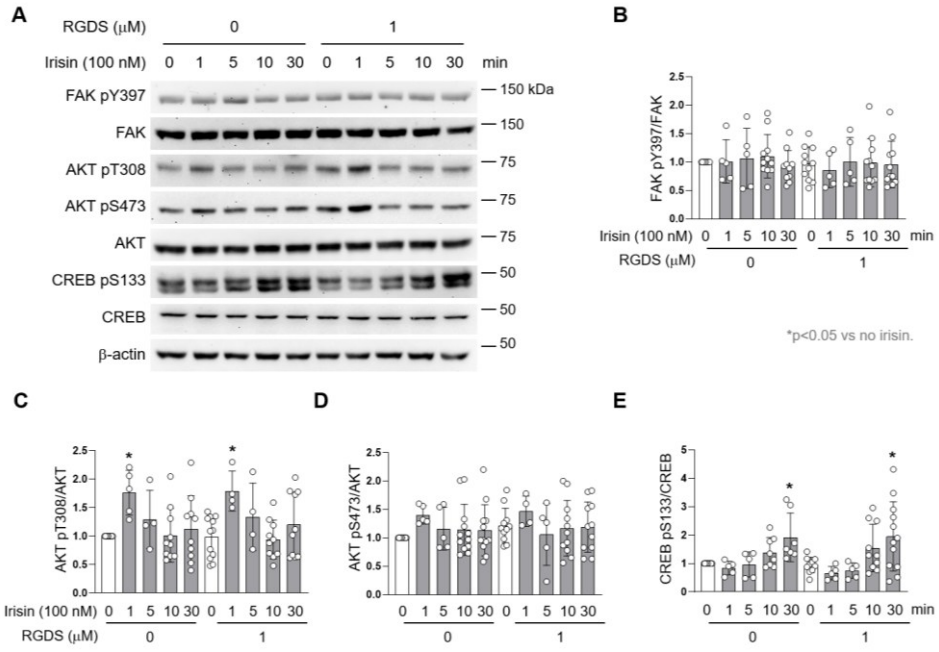

Fig. 3. Irisin signals through an integrin-independent mechanism in pancreatic β-cells. INS-1E cells were pretreated or not with RGDS (1 μmol/l) and subsequently stimulated with recombinant irisin (100 nmol/l) for the indicated time points. Representative immunoblot images showing phosphorylation of FAK at Tyr397, AKT at Thr308 and Ser473, and CREB at Ser133 (**A**). Densitometric analysis of phosphorylated proteins normalized to total FAK (**B**), total AKT (**C, D**), or total CREB (**E**) and expressed relative to untreated controls (**B–E**). Data are presented as mean ± SD. *P < 0.05. Statistical analysis was performed using two-way ANOVA with Sidak's and Tukey's post hoc tests or one-way ANOVA with Sidak's post hoc test.

4.3 Irisin promotes insulin secretion through an integrin-independent mechanism

To confirm that irisin was able to exert its main biological effect in pancreatic β-cells, we evaluated its ability to promote GSIS in the presence of RGDS, or siRNA directed against integrin αV (#ITGAV). INS-1E cells were treated or not with 1 μmol/l RGDS for 10 min (**Fig. 4A**) or transfected with 30 nmol/l siRNA #ITGAV for 24 h (**Fig. 4B**) and subsequently stimulated with 100 nmol/l irisin for 1 h. GSIS was then assessed after 1 h of incubation at either 3 mmol/l or 25

mmol/l glucose (**Fig. 4A, B**). Insulin secretion was normalized to total protein content and expressed as the stimulation index (25 mmol/l/3 mmol/l GSIS).

Figure 4. Irisin promotes insulin secretion through an integrin-independent mechanism

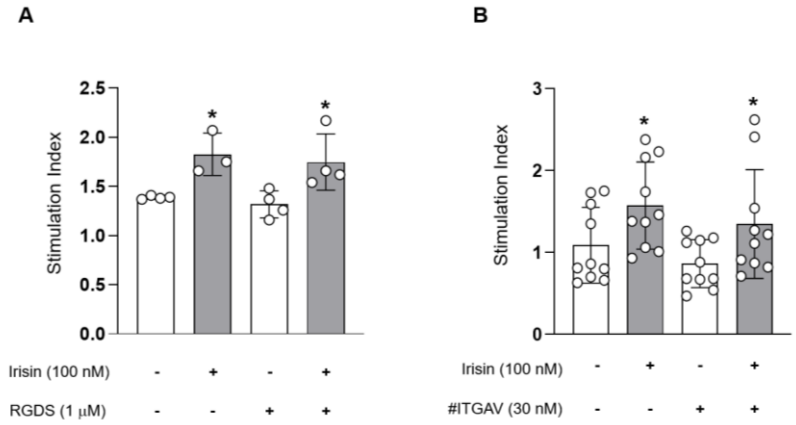

Figure 4. Irisin promotes insulin secretion through an integrin-independent mechanism. INS-1E cells were treated or not with the integrin inhibitor RGDS (1 μmol/l) for 10 min (**A**) or transfected with siRNA targeting integrin αV (siRNA #ITGAV, 30 nmol/l) for 24 h (**B**), and subsequently stimulated with recombinant irisin (100 nmol/l) for 1 h. GSIS was assessed following 1 h of incubation at low (3 mmol/l) or high (25 mmol/l) glucose concentrations. Insulin secretion was normalized to total protein content and expressed as the stimulation index (25 mmol/l / 3 mmol/l glucose).

4.4 Identification of irisin receptor candidates in human pancreatic islets

To identify potential irisin receptors in pancreatic β-cells, a pull-down assay coupled to MS analysis was performed using human pancreatic islet lysates (**Fig. 5A-C**). C-terminal His-tagged irisin was used as bait, and proteins specifically co-eluted with irisin were identified by quantitative proteomics, using appropriate negative and positive controls. Comparative analysis revealed a total of 102 proteins specifically enriched in the irisin pull-down compared with controls (**Fig. 5B-C**). However, none of the identified proteins exhibited known receptor functions, suggesting that irisin does not directly interact with a classical cell-surface receptor detectable by this approach in human pancreatic islets.

Figure 5. Identification of irisin receptor candidates in human pancreatic islets

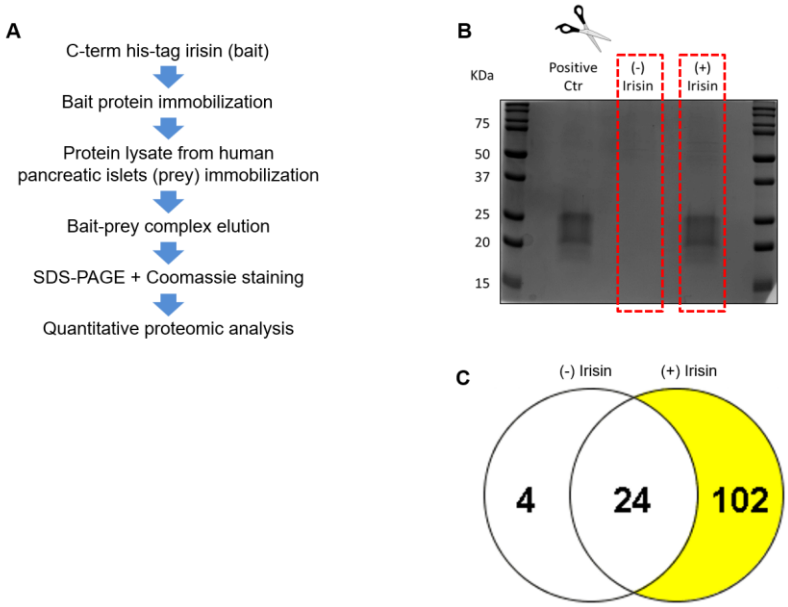

Fig. 5. Identification of irisin receptor candidates in human pancreatic islets. Pull-down assay/MS approach (**A–C**). Schematic representation of the pull-down/MS workflow used to identify irisin interactors in human pancreatic islets (**A**). Briefly, 100 µg of C-terminal His-tagged irisin [(+) irisin] were immobilized on HisPur™ Cobalt chelate affinity resin. Resin without irisin [(-) irisin] was used as a negative control. Human pancreatic islet protein lysates (800 µL) were incubated with both (+) irisin and (−) irisin resins. Resin loaded with His-tagged irisin but not incubated with islet lysate served as a positive control. After extensive washing, irisin-interactor complexes were eluted using an imidazole-containing buffer. Eluted proteins were precipitated, resuspended in NuPAGE™ LDS sample buffer containing DTT, and resolved by 12% SDS-PAGE followed by Coomassie Blue staining. Lanes corresponding to the (−) irisin and (+) irisin conditions were subsequently subjected to quantitative proteomic analysis (**B**). Venn diagram showing the number of proteins specifically co-eluted with irisin (**C**).

4.5 Gene Ontology analysis: Cellular Component

To explore potential functional relationships among the proteins co-eluted with irisin, the identified protein set was analyzed using the STRING database. Functional enrichment analysis of the resulting interaction network revealed a significant overrepresentation of GO terms associated with specific biological processes and molecular functions (**Tab.3**). Enrichment was evaluated based on

the number of proteins within the network annotated with each GO term "*Count in network*" and the corresponding enrichment strength, expressed as the log10 ratio of observed versus expected proteins. Several GO categories showed significant enrichment after correction for multiple testing, as indicated by a low FDR. As shown in the table (**Tab.3**), the most significantly enriched "*Cellular Component*" GO terms in the protein network were related to intracellular compartments and, in particular, included vesicles and lipid-rafts, both of which are critically involved in endocytic processes. Based on these findings, we hypothesized that irisin may undergo cellular internalization in pancreatic β-cells.

Table 3. GO analysis: Cellular Component

Cellular Component (Gene Ontology)				
GO-term	*Description*	*Count in network*	*Strenght*	*False discovery rate*
GO:0005737	cytoplasm	89 of 11238	0.21	5.26E-12
GO:0005622	intracellular	91 of 14286	0.11	1.88E-06
GO:0005829	cytosol	47 of 4958	0.29	2.46E-05
GO:0043227	membrane-bounded organelle	78 of 11244	0.15	2.76E-05
GO:0043229	intracellular organelle	81 of 12193	0.13	5.69E-05
GO:0043231	intracellular membrane-bounded organelle	73 of 10365	0.16	7.17E-05
GO:0031982	**vesicle**	**25 of 2318**	**0.34**	**0.0011**
GO:0045121	**membrane raft**	**8 of 300**	**0.74**	**0.0012**

Tab. 3. GO analysis: Cellular Component. Functional enrichment analysis of proteins co-eluted with irisin was performed using the STRING database. GO terms were analyzed to identify overrepresented cellular components, biological processes, and molecular functions within the interaction network. Enrichment was evaluated based on the number of proteins annotated with each term ("count in network"), enrichment strength (log10 observed/expected), and FDR-corrected p-values.

4.6 Irisin is endocytosed in INS-1E cells

To explore the hypothesis that irisin is effectively internalized by pancreatic β-cells, INS-1E cells were treated or not with recombinant 100 nmol/l irisin for different time points (**Fig.6A-B**). After stimulation, the culture medium was removed, cells were extensively washed, and intracellular proteins were analyzed by immunoblotting. Under basal conditions, INS-1E cells showed no detectable irisin signal, whereas irisin-treated cells displayed a specific protein band, indicating that irisin was internalized (**Fig.6A**). These findings were further confirmed by immunofluorescence analysis, which revealed an increased

intracellular signal following irisin stimulation, predominantly localized within the cytoplasm (**Fig.6B**).

Several studies have demonstrated that denatured or structurally altered proteins fail to undergo efficient cellular internalization, particularly when uptake relies on specific ligand-receptor interactions rather than nonspecific fluid-phase endocytosis (34,35). Accordingly, disruption of protein folding, chemical modification, or improper post-translational processing can markedly impair ligand binding and subsequent endocytic trafficking (36,37). In line with this concept, recent evidence indicates that the biological activity and receptor engagement of irisin are strongly influenced by its structural conformation and post-translational modifications (18,25), supporting the notion that protein integrity is required for efficient irisin internalization.

Based on this evidence, we next investigated whether heat-denatured irisin retained the ability to be internalized by pancreatic β-cells. To this end, INS-1E cells were treated or not with 100 nmol/l native irisin or heat-denatured irisin (boiled at 99 °C for 10 min). Immunoblotting analysis revealed that heat-denatured irisin was no longer detectable within the cells, indicating a loss of internalization capacity, whereas native irisin remained efficiently internalized. These findings provide the first experimental evidence supporting a structure-dependent mechanism of irisin uptake in pancreatic β-cells and are consistent with the in silico functional enrichment analysis previously performed using the STRING database (**Fig.6C**).

In mammalian cells, multiple and partially redundant endocytic pathways coexist. Importantly, inhibition of a single pathway can often be compensated by alternative endocytic routes, complicating the identification of the predominant mechanism responsible for ligand internalization (38–40).

Based on this notion, INS-1E cells were treated with different pharmacological inhibitors targeting distinct endocytic pathways to investigate the mechanism underlying irisin internalization (data not shown). Among all the inhibitors

tested, only nystatin, an inhibitor of cholesterol-dependent, lipid raft-mediated endocytosis, significantly reduced irisin uptake in INS-1E cells, as assessed by immunoblotting analysis (**Fig.6D**). These results may suggest that irisin internalization in pancreatic β-cells primarily relies on a lipid raft-dependent endocytic mechanism. The effect of nystatin on GSIS could not be evaluated, as prolonged nystatin treatment resulted in significant cytotoxicity in INS-1E cells, precluding functional assessment under these conditions.

Figure 6. Irisin is endocytosed in INS-1E cells

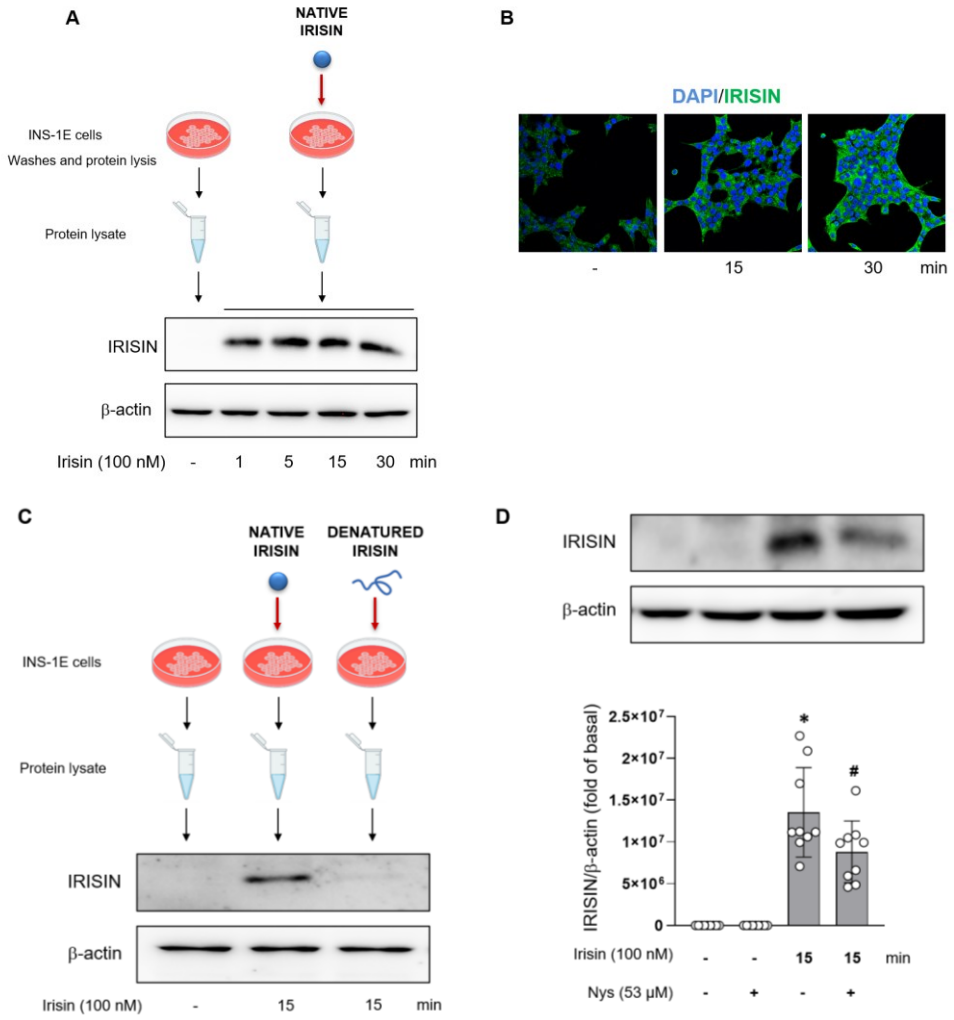

Fig. 6. Irisin is endocytosed in INS-1E cells. INS-1E cells were treated or not with recombinant irisin (100 nmol/l) for the indicated time points **(A-B)**. After stimulation, cells were extensively washed and analyzed for intracellular irisin by immunoblotting (**A**) and immunofluorescence microscopy (**B**). INS-1E cells were treated with native or heat-denatured irisin (100 nmol/l; 99 °C for 10 min). Intracellular irisin levels were assessed by immunoblotting (**C**). INS-1E cells were pretreated with nystatin (53 µmol/l) for 1 hour, followed by stimulation with irisin (100 nmol/l) for 15 minutes. Cells were then lysed for immunoblot analysis. Immunoblot images were used to assess intracellular irisin levels (**D**). Data are presented as mean ± SD. *P < 0.05. Statistical analysis was performed using two-way ANOVA with Sidak's and Tukey's post hoc tests or one-way ANOVA with Sidak's post hoc test.

4.7 His-tag irisin is not endocytosed in INS-1E cells, and it is not able to increase GSIS

In contrast to native irisin, cellular internalization could not be detected by either immunoblotting or immunofluorescence when INS-1E cells were stimulated or not with 100 nmol/l His-tagged irisin for different time points (**Fig.7A, B**).

To further investigate the functional relevance of endocytosis in irisin biological activity, we next assessed whether His-tagged irisin, despite its inability to undergo cellular internalization, was able to promote GSIS to an extent comparable to native irisin. As shown in the graph, His-tagged irisin failed to enhance GSIS, in contrast to untagged irisin (**Fig.7C**). These findings indicate that irisin internalization is required for its insulinotropic effect in pancreatic β-cells.

Figure 7. His-tag irisin is not endocytosed in INS-1E cells, and it is not able to increase GSIS

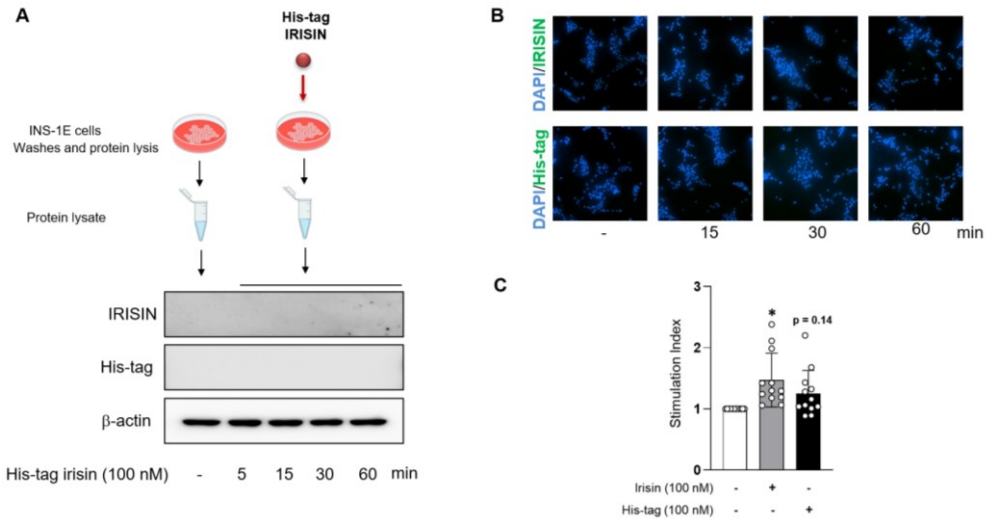

Fig. 7. His-tag irisin is not endocytosed in INS-1E cells, and it is not able to increase GSIS. INS-1E cells were treated or not with His-tagged irisin (100 nmol/l) for the indicated time points (**A–B**). Intracellular irisin levels were assessed by immunoblotting following extensive washing and cell lysis (**A**). Cellular localization of His-tagged irisin was evaluated by immunofluorescence analysis (**B**). In both immunoblotting and immunofluorescence assays, the absence of intracellular irisin signal was consistently confirmed using either an anti-irisin antibody or an anti–His-tag antibody. To assess the insulinotropic activity of His-tagged irisin, INS-1E cells were stimulated with 100 nmol/l His-tagged or untagged irisin,

and GSIS was measured after incubation at 3 mmol/l or 25 mmol/l glucose. Insulin secretion was normalized to total protein content and expressed as stimulation index (25/3 mmol/l glucose). Data are presented as mean ± SD. *$p < 0.05$. Statistical analysis was performed using one-way or two-way ANOVA with appropriate post hoc tests, as indicated.

4.8 Irisin binds to the plasma membrane before being internalized in INS-1E cells

INS-1E cells were incubated with 6 µg/µl TriCEPS conjugated to 1 µg/µl recombinant irisin to evaluate irisin binding to its putative cell-surface receptor under different experimental conditions, including temperature, incubation time, and pH (**Fig. 8A-B**). In this preliminary assay, transferrin, used as a positive control, displayed a pronounced fluorescence shift (red peak), consistent with binding to its widely expressed cell-surface receptor, whereas glycine (blue peak), used as a negative control, overlapped with the background fluorescence (purple peak), confirming assay specificity (**Fig. 8B**).

Flow cytometry analysis showed that optimal ligand binding was achieved under condition 4 (37 °C, 30 min, pH 7.4), as indicated by a clear rightward shift of the fluorescence peak corresponding to irisin-treated cells (green peak) compared with the background control (phycoerythrin–streptavidin alone, purple peak). This shift reflects an increased proportion of cells exhibiting higher fluorescence intensity, consistent with specific binding of the irisin-TriCEPS complex to the cell surface. In contrast, under conditions 1 (22 °C, 30 min, pH 7.4) and 2 (4°C, 90 min, pH 7.4), the irisin-associated fluorescence peaks largely overlapped with the background signal, indicating weak or non-specific binding, whereas condition 3 (4°C, 90 min, pH 6.5) showed poorly defined peaks together with evident signs of cellular stress, preventing reliable interpretation (**Fig. 8B**).

Figure 8. Irisin binds to the plasma membrane before being internalized in INS-1E cells

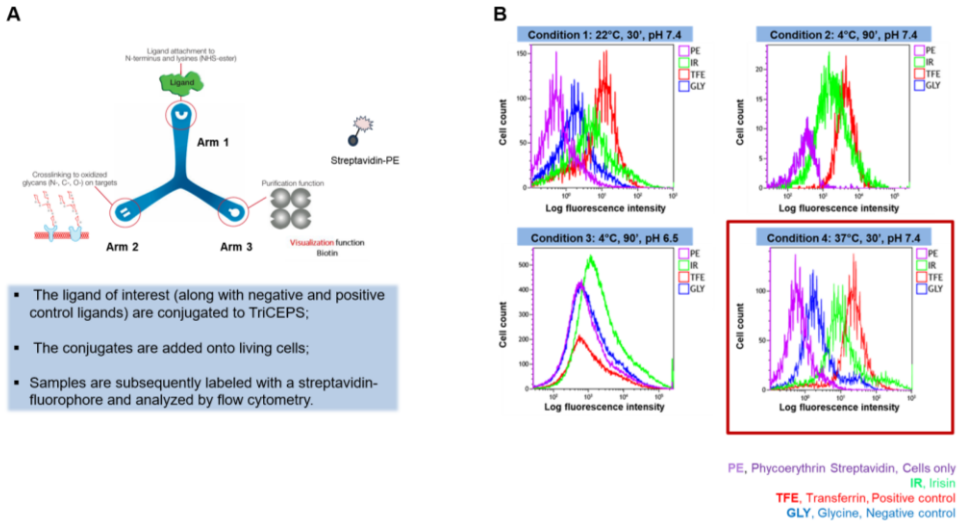

Fig. 8. Irisin binds to the plasma membrane before being internalized in INS-1E cells. Schematic representation of the preliminary test flow-TriCEPS technology (**A**). INS-1E cells were incubated with TriCEPS (6 µg/µl) conjugated to recombinant irisin (1 µg/µl) to evaluate irisin binding to putative cell-surface components under different experimental conditions of temperature (4 °C, 22 °C, or 37 °C), incubation time (30 or 90 min), and pH (7.4 or 6.5). Transferrin, a ligand whose receptor is widely expressed on the cell membrane, was used as a positive control, whereas glycine, whose receptor is poorly expressed on the cell surface, was used as a negative control. Cells incubated with phycoerythrin-streptavidin alone were included as a control for background fluorescence (**B**). Binding was analyzed by flow cytometry, and fluorescence intensity was displayed on a logarithmic scale. Data are presented as the number of cells positive for the fluorescence signal plotted against fluorescence intensity.

4.9 Irisin protein targets on INS-1E cell plasma membrane

Based on the preliminary test flow-TriCEPS results, the main LRC-TriCEPS experiment was performed, following the manufacturer's instructions, and using the optimized binding condition (37°C, 30 min, pH 7.4) (**Fig.9**).

Figure 9. Overview of the LRC-TriCEPS workflow.

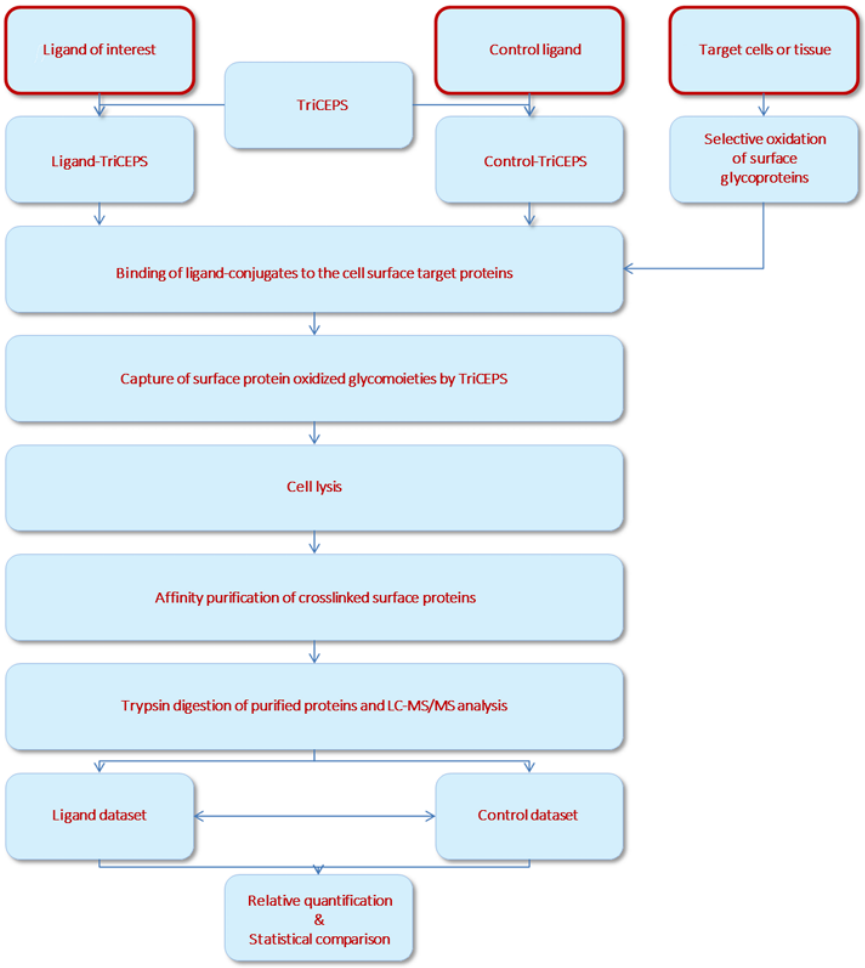

Fig.9. Flow chart of the LRC-TriCEPS experiment using TriCEPS reagent.

A total of 501 surface associated proteins were confidently identified by LC-MS/MS. The results are shown as a volcano plot (**Fig.10, 11, 12**). A volcano plot combines a measure of statistical significance from a statistical test (in this case adjusted p-value from an ANOVA model) with the magnitude of the change, enabling quick visual identification of proteins that display changes that are also

statistically significant. The x-axis represents the mean ratio fold change (on a log2 scale). The y-axis represents the statistical significance p-value of the ratio fold change for each protein (on a -log10 scale). Proteins that are enriched in one of the sample sets (triplicate), will plot either left or right of the x-axis origin, indicating in which sample set that protein is enriched. The criteria to consider a protein as a candidate for interacting to the ligand of interest are the following: FDR >0.05 and S curve = 0.5.

In the following plots, data is shown at the protein level and proteins were annotated using the rat proteome database from Uniprot. Results were filtered for surface associated proteins.

The transferrin receptor (TFR1), the known target of transferrin (TRFE), was clearly enriched in the TRFE samples indicating the technical success of the experiment. In addition, no proteins were enriched in the negative control samples (GLY) when compared to TRFE indicating the specificity of the experiment (**Fig. 10, Tab. 4**).

Figure 10. Volcano plot depicting the comparison between the glycine and the transferrin samples

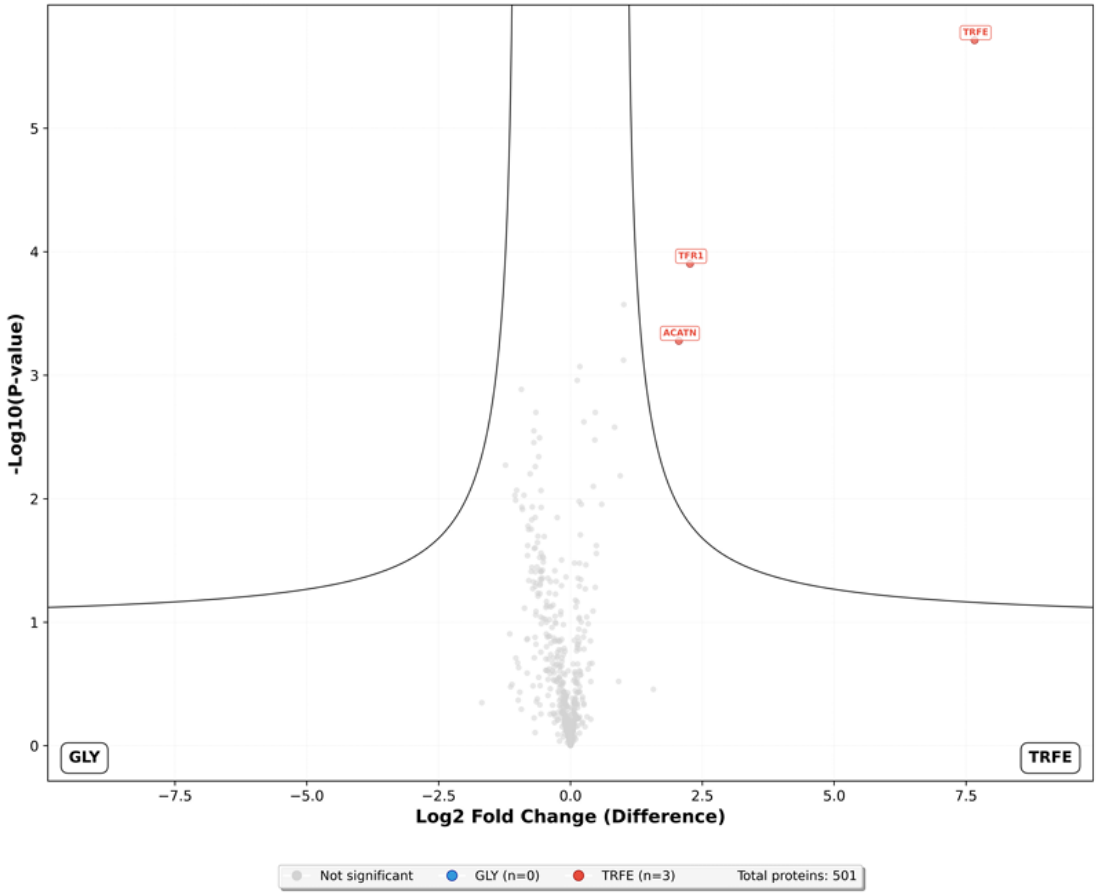

Fig. 10. Volcano plot depicting the comparison between the Glycine and the Transferrin samples. TFR1 is clearly enriched in the TRFE samples. Protein ACATN is a known impurity of TRFE. Results are presented in the format of a volcano plot: Y axis = -Log10 (adj. p-value), X-axis = Log2 fold change compared to the other sample. The points in the white space indicate candidate targets that display both large magnitude fold-changes (x axis) and high statistical significance (-Log10 of adjusted p-value, y axis).

Table 4. Proteins enriched in corresponding samples.

Enriched in	Protein Name	Protein ID	Description	log2(FC)	-LOG10(Adj.pvalue)	Annotation
TRFE	TRFE	P12346	Serotransferrin	7.7	5.7	
TRFE	TFR1	Q99376	Transferrin receptor protein 1	2.3	3.9	
TRFE	ACATN	Q6AYY8	Acetyl-coenzyme A transporter 1	2.1	3.3	

	Ligand
	Known receptor
	Contaminant

Several proteins were enriched in the irisin samples, compared to TRFE samples, and they can be considered as candidate targets (**Fig.11, Tab.5**).

Figure 11. Volcano plot depicting the comparison between the irisin and the transferrin samples

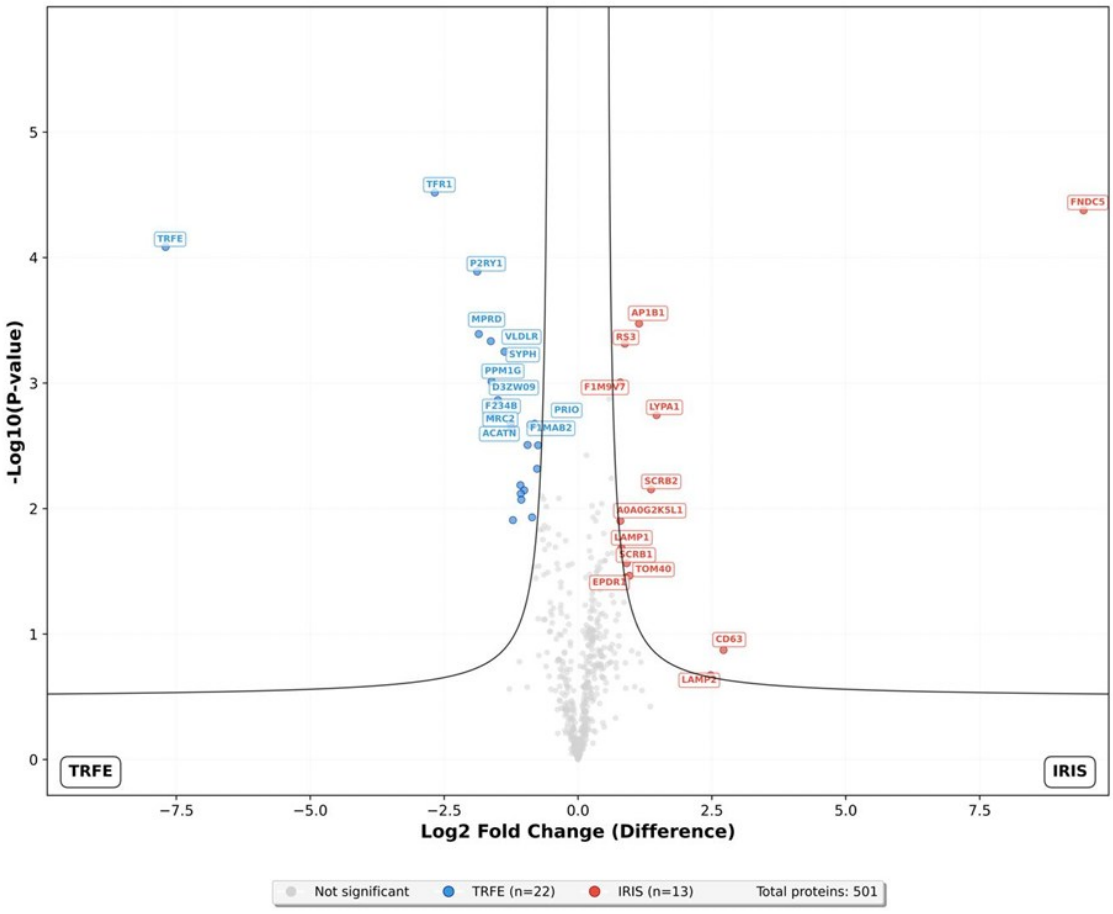

Fig. 11. Volcano plot depicting the comparison between the irisin and the transferrin samples. TFR1, the known target of TRFE, was clearly enriched in the TRFE samples. FNDC5 was also very abundant in the corresponding samples.

Table 5. Proteins enriched in Irisin samples compared to TRFE

Enriched in	Protein Name	Protein ID	Description	log2(FC)	-LOG10(p-VALUE)	Annotation
IRIS	FNDC5	Q8K3V5	Fibronectin type III domain-containing protein 5	9.44	4.38	
IRIS	AP1B1	P52303	AP-1 complex subunit beta-1	1.14	3.47	
IRIS	RS3	P62909	Small ribosomal subunit protein uS3	0.87	3.31	
IRIS	F1M9V7	F1M9V7	Aminopeptidase	0.79	3.01	
IRIS	LYPA1	P70470	Acyl-protein thioesterase 1	1.46	2.75	
IRIS	SCRB2	P27615	Lysosome membrane protein 2	1.36	2.15	
IRIS	A0A0G2K5L1	A0A0G2K5L1	FAT atypical cadherin 1	0.79	1.9	
IRIS	LAMP1	P14562	Lysosome-associated membrane glycoprotein 1	0.81	1.69	
IRIS	SCRB1	P97943	Scavenger receptor class B member 1	0.91	1.56	
IRIS	TOM40	Q75Q40	Mitochondrial import receptor subunit TOM40 homolog	0.96	1.47	
IRIS	EPDR1	Q5XII0	Mammalian ependymin-related protein 1	0.89	1.45	
IRIS	CD63	P28648	CD63 antigen	2.72	0.87	
IRIS	LAMP2	P17046	Lysosome-associated membrane glycoprotein 2	2.48	0.67	
TRFE	TFR1	Q99376	Transferrin receptor protein 1	-2.68	4.52	
TRFE	TRFE	P12346	Serotransferrin	-7.7	4.08	
TRFE	P2RY1	P49651	P2Y purinoceptor 1	-1.88	3.89	
TRFE	MPRD	Q6AY20	Cation-dependent mannose-6-phosphate receptor	-1.86	3.39	
TRFE	VLDLR	P98166	Very low-density lipoprotein receptor	-1.63	3.33	
TRFE	SYPH	P07825	Synaptophysin	-1.37	3.25	
TRFE	PPM1G	F1LNI5	Protein phosphatase 1G	-1.62	3.01	
TRFE	D3ZW09	D3ZW09	VPS10 domain-containing receptor SorCS2	-1.5	2.86	
TRFE	F234B	D3ZWJ9	Protein FAM234B	-1.6	2.73	
TRFE	MRC2	Q4TU93	C-type mannose receptor 2	-1.26	2.68	
TRFE	F1MAB2	F1MAB2	Endosome/lysosome-associated apoptosis and autophagy regulator 1	-0.81	2.68	
TRFE	PRIO	P13852	Major prion protein	-0.89	2.67	
TRFE	ACATN	Q6AYY8	Acetyl-coenzyme A transporter 1	-1.24	2.64	
TRFE	LDLR	P35952	Low-density lipoprotein receptor	-0.94	2.51	
TRFE	A0A8I6ABU1	A0A8I6ABU1	Metal cation symporter ZIP14	-0.75	2.5	
TRFE	A0A8I6AUR9	A0A8I6AUR9	Large neutral amino acids transporter small subunit 4	-0.76	2.32	
TRFE	LRP1	G3V928	Prolow-density lipoprotein receptor-related protein 1	-1.08	2.19	
TRFE	LCAP	P97629	Leucyl-cystinyl aminopeptidase	-1.01	2.15	
TRFE	CD151	Q9QZA6	CD151 antigen	-1.07	2.12	
TRFE	A0A8I5ZXH4	A0A8I5ZXH4	Sodium/calcium exchanger 1	-1.06	2.07	
TRFE	S38A1	Q9JM15	Sodium-coupled neutral amino acid symporter 1	-0.86	1.93	
TRFE	PACC1	Q66H28	Proton-activated chloride channel	-1.22	1.91	

Ligand	
Known receptor	
Contaminant	
Candidate target	
Potential downregulated protein	
Common in Gly & TRFE	

Figure 12. Volcano plot depicting the comparison between irisin and glycine samples

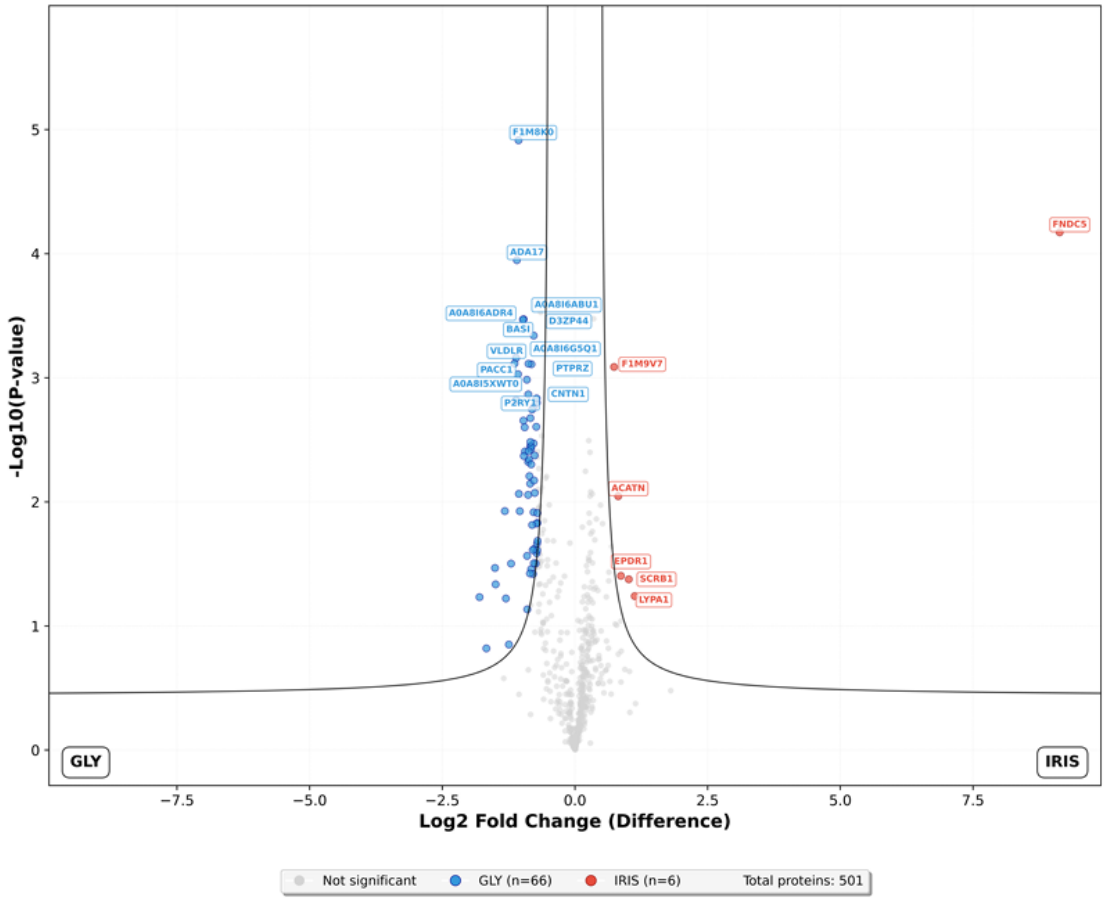

Fig. 12. Volcano plot depicting the comparison between Irisin and Glycine samples.

Table 6. Proteins enriched in irisin samples compared to glycine

Enriched in	Protein Name	Protein ID	Description	log2(FC)	-LOG10(p-VALUE)	Annotation
IRIS	FNDC5	Q8K3V5	Fibronectin type III domain-containing protein 5	9.13	4.17	
IRIS	F1M9V7	F1M9V7	Aminopeptidase	0.74	3.09	
IRIS	ACATN	Q6AYY8	Acetyl-coenzyme A transporter 1	0.81	2.05	
IRIS	EPDR1	Q5XII0	Mammalian ependymin-related protein 1	0.86	1.4	
IRIS	SCRB1	P97943	Scavenger receptor class B member 1	1.01	1.38	
IRIS	LYPA1	P70470	Acyl-protein thioesterase 1	1.12	1.24	

Ligand
Known receptor
Contaminant
Candidate target
Potential downregulated protein

FNDC5 was clearly abundant in the corresponding samples. Several proteins were enriched in the irisin samples which can be considered as candidate targets (**Fig. 11, 12 and Tab. 5, 6**). Notably proteins F1M9V7, EPDR1, SCRB1 and LYPA1 were enriched in the irisin samples against both comparisons.

5. Discussion

T2D is characterized by a progressive decline in pancreatic β-cell functional mass, ultimately leading to impaired glycemic control and chronic metabolic complications. Although current antidiabetic therapies effectively target hyperglycemia and insulin resistance, they only partially address the progressive loss of β-cell function and mass. In this context, identifying novel molecules capable of preserving β-cell integrity and restoring insulin secretory capacity remains a major unmet clinical need. Irisin, a myokine released in response to physical activity and nutritional cues, has emerged as a promising candidate due to its reported ability to promote β-cell survival, proliferation, and GSIS (11,12,22).

In the present study, we investigated the upstream mechanisms mediating irisin action in pancreatic β-cells, focusing on receptor engagement, intracellular signaling, and cellular trafficking. Although integrin αV/β5 has been identified as a functional irisin receptor in bone and adipose tissue (17,18), our data demonstrate that irisin signaling in pancreatic β-cells occurs through an integrin-independent mechanism. Despite the clear expression of integrin αV in both human and rodent β-cells and in human and murine islets, irisin failed to activate the canonical integrin signaling mediator FAK. Moreover, chemical inhibition of integrins using RGDS or knockdown of integrin αV did not interfere with irisin-induced AKT and CREB phosphorylation or with its insulinotropic effect. Together, these findings strongly argue against a functional role for integrins in mediating irisin signaling in pancreatic β-cells and support the concept that irisin employs tissue-specific mechanisms of action (13,22).

From a mechanistic standpoint, integrin-mediated signaling is classically associated with activation of the FAK–PI3K–PDK1 axis, leading to AKT phosphorylation. Upon integrin engagement, FAK acts as a proximal scaffold linking integrins to PI3K activation, resulting in the generation of phosphatidylinositol (3,4,5)-trisphosphate (PIP3) and subsequent recruitment of PDK1 to the plasma membrane, where it directly phosphorylates AKT (41,42).

However, phosphorylation of AKT is not exclusive to integrin signaling but rather reflects activation of PDK1 downstream of PI3K, which can be engaged by multiple upstream mechanisms (43,44).

Importantly, PI3K–PDK1–AKT signaling can also be initiated from cholesterol-rich membrane microdomains and endocytic compartments, independently of integrin engagement. Lipid-rafts and caveolae function as specialized signaling platforms that concentrate PI3K and PIP3, thereby promoting localized PDK1 activation and AKT phosphorylation (45–47).

In this context, the absence of FAK activation together with preserved AKT and CREB phosphorylation in the presence of integrin inhibition strongly indicates that irisin activates a PI3K–PDK1–AKT signaling axis independently of canonical integrin signaling in pancreatic β-cells.

Consistent with this alternative mechanism of action, our initial proteomic pull-down approach performed on human pancreatic islets did not identify classical membrane receptors among the proteins specifically co-eluted with irisin. Instead, GO enrichment analysis revealed a significant overrepresentation of intracellular compartments, particularly vesicles and lipid-rafts, suggesting the involvement of endocytic processes and providing a rationale to directly investigate whether irisin undergoes cellular internalization in pancreatic β-cells.

Indeed, we demonstrate that irisin is effectively internalized by INS-1E cells, as shown by both immunoblotting and immunofluorescence analyses. Irisin was not detectable intracellularly under basal conditions, indicating that the observed signal reflects genuine uptake rather than endogenous expression. These findings are consistent with prior evidence obtained in other cellular contexts, including pulmonary epithelial cells in a translational I/R injury model, in which irisin internalization was mechanistically linked to cytoprotective effects (25).

A key aspect emerging from our data is that irisin internalization depends on protein structural integrity. Receptor-mediated internalization typically requires an intact ligand conformation to ensure productive binding and trafficking;

accordingly, denatured or structurally altered proteins often fail to undergo efficient uptake when internalization depends on specific ligand-target interactions rather than nonspecific fluid-phase endocytosis (35–37,48). In our model, heat-denatured irisin completely lost its ability to be internalized by pancreatic β-cells, further supporting a structure-dependent uptake mechanism.

Endocytosis in mammalian cells occurs through multiple, partially redundant pathways, including clathrin-mediated endocytosis, caveolae- and lipid raft-dependent internalization, and macropinocytosis. Because inhibition of one route may be compensated by others, a stepwise pharmacological strategy is often required to identify the predominant uptake mechanism (38–40). Accordingly, we employed selective inhibitors targeting distinct endocytic routes. Inhibition of dynamin-dependent endocytosis with dynasore or of macropinocytosis with amiloride did not significantly affect irisin internalization, suggesting that these pathways are not primary contributors to irisin uptake in pancreatic β-cells under our experimental conditions.

In contrast, inhibition of cholesterol-dependent endocytosis using nystatin markedly reduced irisin internalization, indicating a predominant role for lipid raft-dependent mechanisms. Nystatin binds membrane cholesterol, thereby disrupting cholesterol-rich microdomains and selectively impairing lipid raft- and caveolae-dependent endocytic pathways without directly affecting clathrin-mediated uptake. Although prolonged nystatin exposure prevented functional assessment of GSIS due to cytotoxicity, the selective loss of irisin internalization alone supports the functional relevance of this pathway. This finding is consistent with both our STRING-based enrichment analysis and previous evidence from pulmonary I/R models, in which irisin uptake and protective effects were similarly sensitive to lipid-rafts disruption (25).

Importantly, our functional data establish a direct link between internalization and insulinotropic activity. His-tagged irisin failed to undergo cellular internalization and was also unable to promote GSIS, despite being present

extracellularly. This dissociation between surface availability and biological activity indicates that intracellular trafficking is required for irisin to exert its effects on insulin secretion and that irisin does not act solely through a classical surface-confined signaling mechanism in pancreatic β-cells.

To further investigate the initial step of irisin action at the plasma membrane, we employed LRC-TriCEPS technology. Flow-TriCEPS preliminary experiments demonstrated that irisin binds the plasma membrane of INS-1E cells under physiological conditions prior to internalization, supporting a two-step model in which irisin first associates with a membrane component and is subsequently internalized. The LRC-TriCEPS main experiment identified a restricted set of surface-associated proteins enriched in irisin-treated samples compared to both transferrin and glycine controls. Notably, among the proteins consistently enriched in irisin samples were F1M9V7, EPDR1, SCRB1 and LYPA1. Although none of these proteins can currently be defined as a classical irisin receptor, their enrichment suggests potential involvement in irisin membrane association, lipid-rafts localization, or endocytic trafficking.

Taken together, our results delineate a novel mechanism of irisin action in pancreatic β-cells characterized by integrin-independent signaling, structure-dependent membrane binding, lipid raft-mediated internalization, and functional reliance on endocytic trafficking. This model expands the current understanding of irisin biology and provides a mechanistic framework to explain its insulinotropic and β-cell-protective effects in a tissue-specific manner.

6. Conclusions

This study provides new insight into the molecular mechanisms underlying irisin action in pancreatic β-cells, demonstrating that irisin exerts its insulinotropic effects through an integrin-independent pathway that critically relies on cellular internalization. While αV integrins have been identified as functional irisin receptors in other tissues, our findings reveal a distinct, tissue-specific mechanism in pancreatic β-cells, characterized by membrane binding followed by lipid raft-dependent endocytosis and activation of PI3K–PDK1–AKT and CREB signaling pathways.

The identification of endocytosis as a prerequisite for irisin-mediated insulin secretion supports the concept that irisin signaling in β-cells is not confined to classical surface receptor activation, but instead requires intracellular trafficking to elicit its biological effects. In line with emerging evidence indicating that irisin action is highly context-dependent and may involve alternative receptors or mechanisms in different cellular systems (3,17,25), our LRC-TriCEPS analyses further suggest the involvement of specific membrane-associated proteins that may participate in irisin binding or internalization.

Together, these findings lay the foundation for future studies aimed at defining the membrane component(s) responsible for irisin recognition and uptake in pancreatic β-cells. Elucidation of this mechanism may open new perspectives for the development of innovative therapeutic strategies designed to preserve β-cell functional mass and counteract disease progression in T2D.

7. References

1.International Diabetes Federation. IDF Diabetes Atlas, 11th edition [Internet]. Brussels, Belgium: International Diabetes Federation; 2025. Report No.: 11th edition. Available from: https://diabetesatlas.org

2.American Diabetes Association Professional Practice Committee. 2. Diagnosis and Classification of Diabetes: Standards of Care in Diabetes-2025. Diabetes Care. 2025 Jan 1;48(1 Suppl 1):S27–49.

3.Młynarska E, Czarnik W, Dzieża N, Jędraszak W, Majchrowicz G, Prusinowski F, et al. Type 2 Diabetes Mellitus: New Pathogenetic Mechanisms, Treatment and the Most Important Complications. Int J Mol Sci. 2025 Jan 27;26(3):1094.

4.Ahmed M, Nofal A, Shafiq A, Javaid H, Ahsan A, Nadeem ZA, et al. Rising mortality rates linked to type-2 diabetes and obesity in the United States: An observational analysis from 1999 to 2022. J Diabetes Investig. 2025 Mar;16(3):492–500.

5.Biondi G, Marrano N, Borrelli A, Rella M, D'Oria R, Genchi VA, et al. The p66Shc Redox Protein and the Emerging Complications of Diabetes. Int J Mol Sci. 2023 Dec 20;25(1):108.

6.Biondi G, Marrano N, Borrelli A, Rella M, Palma G, Calderoni I, et al. Adipose Tissue Secretion Pattern Influences β-Cell Wellness in the Transition from Obesity to Type 2 Diabetes. Int J Mol Sci. 2022 May 15;23(10):5522.

7.Tanday N, Lafferty RA, Flatt PR, Irwin N. Beneficial metabolic effects of recurrent periods of beta-cell rest and stimulation using stable neuropeptide Y1 and glucagon-like peptide-1 receptor agonists. Diabetes Obes Metab. 2022 Dec;24(12):2353–63.

8.Boland BB, Brown C, Boland ML, Cann J, Sulikowski M, Hansen G, et al. Pancreatic β-Cell Rest Replenishes Insulin Secretory Capacity and Attenuates Diabetes in an Extreme Model of Obese Type 2 Diabetes. Diabetes. 2019 Jan;68(1):131–40.

9.Kalwat MA, Scheuner D, Rodrigues-Dos-Santos K, Eizirik DL, Cobb MH. The Pancreatic ß-cell Response to Secretory Demands and Adaption to Stress. Endocrinology. 2021 Nov 1;162(11):bqab173.

10.Marrano N, Biondi G, Cignarelli A, Perrini S, Laviola L, Giorgino F, et al. Functional loss of pancreatic islets in type 2 diabetes: How can we halt it? Metabolism. 2020 Sept;110:154304.

11.Marrano N, Biondi G, Borrelli A, Cignarelli A, Perrini S, Laviola L, et al. Irisin and Incretin Hormones: Similarities, Differences, and Implications in Type 2 Diabetes and Obesity. Biomolecules. 2021 Feb 15;11(2):286.

12.Natalicchio A, Marrano N, Biondi G, Spagnuolo R, Labarbuta R, Porreca I, et al. The Myokine Irisin Is Released in Response to Saturated Fatty Acids and Promotes Pancreatic β-Cell Survival and Insulin Secretion. Diabetes. 2017 Nov;66(11):2849–56.

13.Liu S, Cui F, Ning K, Wang Z, Fu P, Wang D, et al. Role of irisin in physiology and pathology. Front Endocrinol. 2022;13:962968.

14.Marrano N, Biondi G, Borrelli A, Rella M, Zambetta T, Di Gioia L, et al. Type 2 Diabetes and Alzheimer's Disease: The Emerging Role of Cellular Lipotoxicity. Biomolecules. 2023 Jan 16;13(1):183.

15.Huang X, Ren X, Zhao L, Hao Y, Zhao Z, Chen F, et al. Irisin Is a Potential Novel Biomarker and Therapeutic Target Against Kidney Diseases. Cell Biochem Funct. 2025;43(5):e70075.

16.Jenkin KA, Perry BD. Skeletal Muscle and Kidney Crosstalk in Chronic Kidney Disease. Cell Physiol Biochem Int J Exp Cell Physiol Biochem Pharmacol. 2022 Oct 26;56(5):587–601.

17.Kim H, Wrann CD, Jedrychowski M, Vidoni S, Kitase Y, Nagano K, et al. Irisin Mediates Effects on Bone and Fat via αV Integrin Receptors. Cell. 2018 Dec 13;175(7):1756-1768.e17.

18.A M, Wales TE, Zhou H, Draga-Coletă SV, Gorgulla C, Blackmore KA, et al. Irisin acts through its integrin receptor in a two-step process involving extracellular Hsp90α. Mol Cell. 2023 June 1;83(11):1903-1920.e12.

19.de Freitas GB, Lourenco MV, De Felice FG. Protective actions of exercise-related FNDC5/Irisin in memory and Alzheimer's disease. J Neurochem. 2020 Dec;155(6):602–11.

20.Schumacher MA, Chinnam N, Ohashi T, Shah RS, Erickson HP. The structure of irisin reveals a novel intersubunit β-sheet fibronectin type III (FNIII) dimer: implications for receptor activation. J Biol Chem. 2013 Nov 22;288(47):33738–44.

21.Maak S, Norheim F, Drevon CA, Erickson HP. Progress and Challenges in the Biology of FNDC5 and Irisin. Endocr Rev. 2021 July 16;42(4):436–56.

22.Paoletti I, Coccurello R. Irisin: A Multifaceted Hormone Bridging Exercise and Disease Pathophysiology. Int J Mol Sci. 2024 Dec 16;25(24):13480.

23.Decourt C, Evans MC, Inglis MA, Anderson GM. Central Irisin Signaling Is Required for Normal Timing of Puberty in Female Mice. Endocrinology. 2022 Dec 19;164(2):bqac208.

24.Yan W, Chen Y, Guo Y, Xia Y, Li C, Du Y, et al. Irisin Promotes Cardiac Homing of Intravenously Delivered MSCs and Protects against Ischemic Heart Injury. Adv Sci Weinh Baden-Wurtt Ger. 2022 Mar;9(7):e2103697.

25.Chen K, Xu Z, Liu Y, Wang Z, Li Y, Xu X, et al. Irisin protects mitochondria function during pulmonary ischemia/reperfusion injury. Sci Transl Med. 2017 Nov 29;9(418):eaao6298.

26.Liu J, Song N, Huang Y, Chen Y. Irisin inhibits pancreatic cancer cell growth via the AMPK-mTOR pathway. Sci Rep. 2018 Oct 15;8(1):15247.

27.Xue C, Li X, Ba L, Shen Y, Sun Z, Gu J, et al. Irisin mediates beiging of adipose-derived mesenchymal stem cells through binding to TRPC3. BMC Biol. 2022 May 2;20(1):95.

28.Marchetti P, Lupi R, Federici M, Marselli L, Masini M, Boggi U, et al. Insulin secretory function is impaired in isolated human islets carrying the Gly(972)-->Arg IRS-1 polymorphism. Diabetes. 2002 May;51(5):1419–24.

29.Gheibi S, Cataldo LR, Hamilton A, Huang M, Kalamajski S, Fex M, et al. Reduced Expression Level of Protein Phosphatase PPM1E Serves to Maintain Insulin Secretion in Type 2 Diabetes. Diabetes. 2023 Apr 1;72(4):455–66.

30.Kong L, Zhao Q, Jiang X, Hu J, Jiang Q, Sheng L, et al. Trimethylamine N-oxide impairs β-cell function and glucose tolerance. Nat Commun. 2024 Mar 21;15(1):2526.

31.Soffientini P, Bachi A. STAGE-diging: A novel in-gel digestion processing for proteomics samples. J Proteomics. 2016 May 17;140:48–54.

32.Käll L, Canterbury JD, Weston J, Noble WS, MacCoss MJ. Semi-supervised learning for peptide identification from shotgun proteomics datasets. Nat Methods. 2007 Nov;4(11):923–5.

33.Nesvizhskii AI, Keller A, Kolker E, Aebersold R. A statistical model for identifying proteins by tandem mass spectrometry. Anal Chem. 2003 Sept 1;75(17):4646–58.

34.Mukherjee S, Ghosh RN, Maxfield FR. Endocytosis. Physiol Rev. 1997 July;77(3):759–803.

35.Mellman I. Endocytosis and molecular sorting. Annu Rev Cell Dev Biol. 1996;12:575–625.

36.Stahlhut M, Sandvig K, van Deurs B. Caveolae: uniform structures with multiple functions in signaling, cell growth, and cancer. Exp Cell Res. 2000 Nov 25;261(1):111–8.

37.Walsh G. Biopharmaceutical benchmarks 2018. Nat Biotechnol. 2018 Dec;36(12):1136–45.

38.Doherty GJ, McMahon HT. Mechanisms of endocytosis. Annu Rev Biochem. 2009;78:857–902.

39.Mayor S, Pagano RE. Pathways of clathrin-independent endocytosis. Nat Rev Mol Cell Biol. 2007 Aug;8(8):603–12.

40.Sandvig K, Pust S, Skotland T, van Deurs B. Clathrin-independent endocytosis: mechanisms and function. Curr Opin Cell Biol. 2011 Aug 1;23(4):413–20.

41.Guo W, Giancotti FG. Integrin signalling during tumour progression. Nat Rev Mol Cell Biol. 2004 Oct;5(10):816–26.

42.Legate KR, Wickström SA, Fässler R. Genetic and cell biological analysis of integrin outside-in signaling. Genes Dev. 2009 Feb 15;23(4):397–418.

43.Hemmings BA, Restuccia DF. PI3K-PKB/Akt pathway. Cold Spring Harb Perspect Biol. 2012 Sept 1;4(9):a011189.

44.Manning BD, Toker A. AKT/PKB Signaling: Navigating the Network. Cell. 2017 Apr 20;169(3):381–405.

45.Simons K, Toomre D. Lipid rafts and signal transduction. Nat Rev Mol Cell Biol. 2000 Oct;1(1):31–9.

46.Irannejad R, von Zastrow M. GPCR signaling along the endocytic pathway. Curr Opin Cell Biol. 2014 Apr;27:109–16.

47.Villaseñor R, Ozmen L, Messaddeq N, Grüninger F, Loetscher H, Keller A, et al. Trafficking of Endogenous Immunoglobulins by Endothelial Cells at the Blood-Brain Barrier. Sci Rep. 2016 May 6;6:25658.

48.Riezman H, Woodman PG, van Meer G, Marsh M. Molecular mechanisms of endocytosis. Cell. 1997 Dec 12;91(6):731–8.